J. Membrane Biol. 33, 63–108 (1977)

1-Anilino-8-Naphthalenesulfonate: A Fluorescent Probe of Ion and Ionophore Transport Kinetics and Trans-Membrane Asymmetry

Duncan H. Haynes and Philip Simkowitz

Department of Pharmacology, University of Miami Medical School, Miami, Florida 33152

Received 8 July 1976; revised 24 September 1976

Summary. The kinetics of the transport of the 1-anilino-8-naphthalenesulfonate (ANS^-, an anionic fluorescent probe of the membrane surface) across phospholipid vesicle membranes have been studied using a stopped-flow rapid kinetic technique. The method has been used to gain detailed information about the mechanism of transport of this probe and to study ionophore-mediated cation transport across the membrane. The technique has also been exploited to study differences between the inside and outside surfaces of vesicles containing phosphatidyl choline (PC).

The following is a summary of the major conclusions of this study. (a) Binding of ANS^- on the outside surface occurs within times shorter than 100 μsec while permeation occurs in the time range 5–100 sec. (b) Net transport of ANS^- occurs with cotransport of alkali cations. (c) The transport rate is maximal in the region of the crystalline to liquid-crystalline phase transition, and the increase correlates with changes in the degree of aggregation of the vesicles. (d) Incorporation of phosphatidic acid (PA), phosphatidyl ethanolamine (PE) or cholesterol into PC membranes decreases the rate of ANS^- transport. (e) Neutral ionophores (I) of the valinomycin type increase ANS^- permeability in the presence of alkali cations (M^+) by a mechanism involving the transport of a ternary $I-M^+$-ANS^- complex. The equilibrium constants for formation of these complexes and their rate constants for their permeation are presented. The maximal turnover number for ANS^- transport by valinomycin in dimyristoyl PC vesicles at 35 °C was 46 per sec. (f) The partitioning of the ionophore between the aqueous and membrane phases and the rate of transfer of an ionophore from one membrane have been determined in kinetic experiments. (g) A method is described for the detection of $I-M^+$ complexes on the membrane surface by their enhancement effects on ANS^- fluorescence at temperature below the phase transition temperature on "monolayer" vesicles. The apparent stability constants for several $I-M^+$ complexes are given. (h) Analysis of the effect of ionic strength on the ANS^- binding to the inside outside surfaces indicates that the electrostatic surface potential (at fixed ionic strength and surface change) is larger for the inside surface than for the outside surface. (i) Analysis of the dependence of the maximal ANS^- binding for the inside and outside surfaces of vesicles made from PC and a variable mole fraction of PA, PE or cholesterol indicate that the latter three are located preferentially on the inside surface.

Fluorescent probe methods have become increasingly important to the biophysical study of membranes. The fluorescence methods enjoy a several order of magnitude advantage in sensitivity over nuclear magnetic resonance (NMR) methods. Such sensitivity will be necessary for the study of specific biological reactions such as the high-affinity binding to receptors. Many fluorescent probes exhibit an extreme sensitivity to the polarity of the environment as well as reporting molecular motion offering an important advantage over electron spin resonance (ESR), probes whose primary sensitivity is to molecular motion. A final advantage of the fluorescent probe technique is illustrated in the present communication. Fluorescent probes can be used in conjunction with rapid kinetic methods to obtain information about the rates of binding processes, membrane structural changes and, membrane transport.

The most widely-used fluorescent probe to date is 1-anilino-8-naphthalenesulfonate (ANS^-). This anionic probe of the membrane surface shows an inverse relationship between its fluorescent quantum yield and solvent polarity and is thus a very sensitive probe for hydrophobic binding sites. The present communication is the third in a series of four papers dealing with the behavior of ANS^- fluorescence in phospholipid vesicles. In the two previous studies, we showed that ANS^- fluorescence can be used to gain information about structure changes (Haynes & Staerk, 1974) and ion binding and interaction (Haynes, 1974) in phospholipid vesicles. Specifically, we showed that ANS^- can bind between four polar head groups of phosphatidyl choline (PC) and that changes in the number of these binding sites in vesicles made from mixed phospholipids can be analyzed to determine whether the lipids are randomly mixed on the microscopic scale. This was found to be the case for mixtures of phosphatidic acid (PA^-), dimyristoyl phosphatidyl ethanolamine (PE), and cholesterol with dimyristoyl PC. We have also shown that the binding equilibrium of ANS^- is influenced by the electrostatic surface potential, ψ_0, of the membrane and that the probe can be used to register ion binding on the membrane surface (Haynes, 1974).

In the present communication, we use the stopped-flow rapid mixing technique to measure the rate of transport of ANS^- across the vesicle membrane and to distinguish between binding on the inside and outside surfaces. In two of our previous studies we reported quantitative data for monolayer vesicles, ca. 500 Å spheres of organic solvent covered with a monolayer of phospholipid (Träuble & Grell, 1971). We observed quantitatively similar data for bilayer vesicles but did not report their behavior in detail because we were unable to distinguish between effects on the

outside and the inside surface. However, we were able to deduce that ANS$^-$ penetrates the membrane from our observation that the monolayer and bilayer preparations have the same number of ANS$^-$ binding sites per lipid molecule (0.25/PC). This was taken as evidence that the ANS$^-$ can penetrate to the inside surface during the lifetime of the experiment (>20 sec). Since the initiation of this study, the effect of the phase transition on the ANS$^-$ transport has been reported (Tsong, 1975a, b). In the present study, we use the stopped-flow method to report the kinetics of permeation of ANS$^-$. We make use of our ability to distinguish between behavior on the inside and outside surface to gain information about asymmetric distribution of lipids and differences in the dependence of the surface potential on the charge per unit area of the two surfaces.

We first began studying ANS$^-$ binding on phospholipid membranes in hopes of using the probe fluorescence as a quantitative method for detecting cation complexes of neutral valinomycin-type ionophores on the membrane surface. Addition of neutral ionophores to PC vesicle suspensions treated with ANS$^-$ below their phase transition temperature, under which condition the ionophore cannot easily penetrate the membrane, resulted in an enhancement of the probe fluorescence (Haynes, 1972). We present here a quantitative treatment of this phenomenon, giving apparent binding constants for four monovalent cations with four ionophores on the membrane surface. We present evidence that similar ionophore-cation complexes facilitate ANS$^-$ transport through membranes above their phase transition temperature, and discuss the mechanism in detail.

Our work on ANS$^-$ transport kinetics was initiated because we considered the characterization of such time-dependent behavior necessary to the full characterization of the probe. We believe that a fuller knowledge of the transport kinetics of ANS$^-$ through phospholipid membranes will allow one to make more sophisticated interpretations of the functionally-related, time-dependent changes in ANS$^-$ fluorescence in mitochondrial fragments (Azzi *et al.*, 1969), squid axon (Conti, Tasaki & Wanke, 1971) and sarcoplasmic reticulum (Vanderkooi & Martonosi, 1971a, b). Our studies of ANS$^-$ transport kinetics have involved us in a number of seemingly diverse but actually closely interrelated problems. These include cotransport and countertransport of ions, the size of the inner aqueous compartment of the vesicles, the role of aggregation in the creation of transient defects in membrane structure, the relative effects of polar head groups *vs.* hydrocarbon chain perturbations on the transport

reaction, the effect of ion pairing on ionophore affinity and its effect on membrane potentials generated by the ionophores, and differences in composition and surface potential of the inside and outside vesicle surfaces. We will attempt to give a satisfactory accounting of the interrelations between those phenomena, keeping in mind our limitations of space and time and capacity for true understanding. The fourth paper in this series will describe temperature-jump relaxation experiments which extend our analysis to a faster kinetic range ($t_{\frac{1}{2}} \geqq 10$ μsec).

Materials and Methods

1,2-Dimyristoyl-L-lecithin (PC), dimyristoyl-L-ethanolamine (PE) and phosphatidic acid (PA) derived from egg lecithin were obtained from Koch Light Laboratories. Dipalmitoyl-L-PC was purchased from Fluka. These were used without further purification. The details of the preparation of bilayer and "monolayer" vesicles are given in previous publications (Haynes & Staerk, 1974; Lansman & Haynes, 1975). Sonication was performed in the presence of 3 mM KCl unless otherwise noted. All preparations were made and stored at 35 °C except for dipalmitoyl PC (50 °C) and those containing dimyristoyl PE (58 °C). Analysis of ANS^- transport kinetics showed that at least 95 % of the bilayer vesicles are single-shelled. The sources of the ionophores are as reported previously (Cornelius, Gärtner & Haynes, 1974).

Equilibrium fluorescence and light scattering experiments were performed on a Perkin Elmer Fluorescence Spectrophotometer MPF-3L. Rapid mixing experiments were performed with an Aminco-Morrow Stopped-Flow Apparatus (Cat. No. 4-8409) with the excitation monochromator set at 368 nm and with a Schott GG420 cutoff filter placed in front of the photomultiplier. Mixing was achieved within 10 msec. The "instantaneous" reaction amplitude (A_o) was determined as the difference between the total fluorescent signal at $t = \infty$ (corrected for ca. 5 % light scattering contribution) and the amplitude of the reaction (A_i).

Results and Discussion

Basic Phenomenon

Rapid mixing of phosphatidyl choline (PC) vesicles and ANS^- above the lipid crystalline to crystalline phase transition temperature results in a fluorescence increase which has two kinetic components: (a) An "instantaneous" fluorescence increase (A_o) which occurs within the dead time of the instrument (ca. 1 msec) and (b) a further increase (A_i) with an exponential time course and with a half-time ($t_{\frac{1}{2}}$) of between 5 and 100 sec. We have made these observations for lipid concentrations between 10^{-5} and 10^{-4} M and ANS^- concentrations between 10^{-5} and 10^{-3} M. The

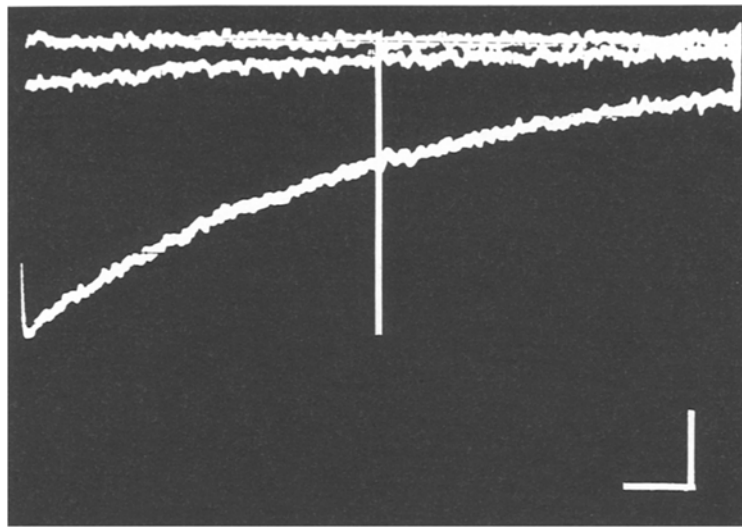

Fig. 1. Stopped-flow trace of ANS^- permeation facilitated by monactin. Time base, 0.5 sec/cm with repetitive sweep; vertical axis 0.2 V/cm (arbitrary); scale markers represent one cm. The vertical line represents the amplitude A_i. Syringe *A* contained 3.3 $\times 10^{-4}$ M dimyristoyl PC vesicles, 4.0×10^{-6} M monactin, 1 mM KCl, 1 mM histidine buffer, pH 7.4. Syringe *B* contained 6.3×10^{-5} M ANS^- and 0.2 M KCl

rate of the slow process is increased by the addition of valimonycin-type ionophores. A typical stopped-flow progress curve of the slow reaction is shown in Fig. 1.

Our interpretation of the slow reaction as a transport phenomenon is illustrated in Fig. 2. In a previous study (Haynes & Staerk, 1974) we have shown that the binding of ANS^- on the surface of monolayer vesicles can be described as

$$ANS^-_{aq} + B \underset{k_{-1}}{\overset{k_1}{\rightleftharpoons}} ANS^- - B \tag{1}$$

where *B* represents a binding site composed of four lecithin polar head groups (*cf.* Haynes & Staerk, 1974). Above the phase transition temperature k_1 has a value of ca. 2×10^8 M^{-1} sec^{-1}. This allows us to estimate that the $t_{\frac{1}{2}}$ value for the binding on the outside surface of the bilayer vesicle will be approximately 10^{-4} sec and that the reaction will appear to be "instantaneous" in the stopped-flow experiment.

The slower kinetic process has been reported by (Tsong, 1975*a*, *b*) to be the transfer of ANS^- across the membrane. His assignment was made from comparisons of the total fluorescence obtained after cosonication of

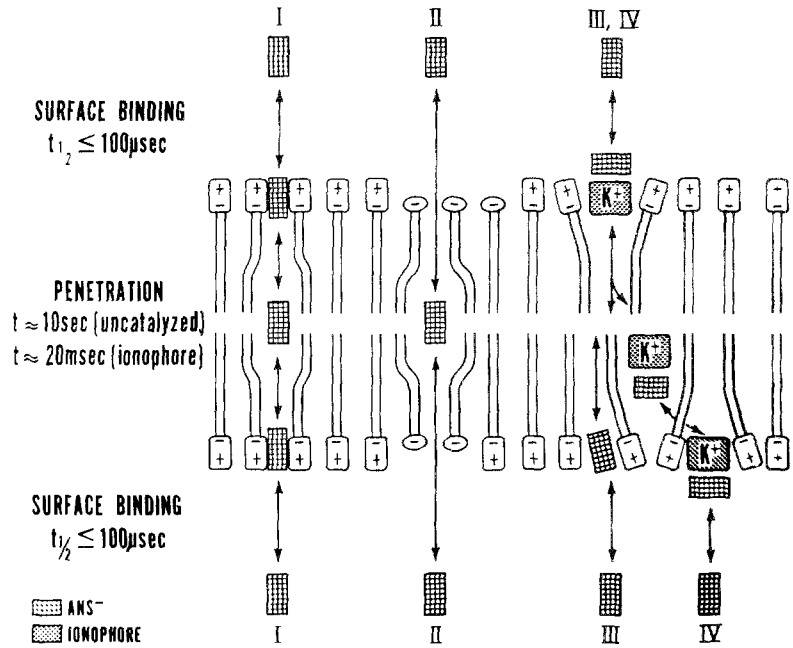

Fig. 2. Permeability mechanisms for ANS^-. (*I*) ANS^- binds to the polar head group region. Penetration of the membrane takes place concomitantly with a structural change in the hydrocarbon chain region. The ANS^- is considered to have only a transient existence in this environment. The ANS^- is transferred to another binding site (if present) on the other side of the membrane and is released to the inner aqueous phase. (*II*) Penetration takes place independently of the polar head group in cases where the latter does not support binding. For models (*I*) and (*II*), M^+ is considered to copermeate, although its mechanism is not shown. (*III*) ANS^- transport occurs by binding in a region perturbed by an ionophore followed by transport through this perturbed region. (*IV*) ANS^- transport occurs strictly by the mechanism of ion pairing with $I-M^+$, followed by cotransport of the ternary complex.

ANS^- and vesicles with that obtained above the phase transition temperature, and by comparisons of the amplitudes of the slow reaction obtained above and below the phase transition temperature. His findings on the effect of the phase transition were corroborated in a study by Jacobson and Papahadjopoulos (1976). We offer three additional arguments in support of his conclusions:

The first observation is that the rate of the slow process is increased by the addition of valinomycin-type ionophores. The second observation is that the amplitude of the slow process decreases with increasing lipid concentration for a low and constant ANS^- concentration. An explanation for this is developed below. Our previous study (Haynes & Staerk, 1974) has shown that the equilibrium ratio of ANS^- bound ($[ANS]_b$) to

the total ANS^- ($[ANS^-]_t$) depends on the concentration of unoccupied binding sites according to the following saturation equation:

$$[ANS]_b/[ANS]_t = K_1[B]/(1+K_1[B]). \tag{2}$$

The reaction amplitude A_i for binding of the probe on the inside surface would be given as:

$$A_i = A_{\text{total}} - A_o = \frac{K_1([B]_o+[B]_i)}{1+K_1([B]_o+[B]_i)} - \frac{K_1[B]_o}{1+K_1[B]_o} \tag{3}$$

where B_i and B_o refer to the binding sites on the inside and outside surfaces of the membrane, respectively. The A quantities are identical to the fraction of maximal ANS^- binding values given in Eq. (2) with the appropriate subscripts for the $[B]$ values. Eq. (3) predicts that the reaction amplitude will first increase, reach a maximum and decrease with increasing lipid concentration (increasing $[B]_o$) tending toward zero when the lipid concentration is very high. This behavior is what is observed experimentally.

The third observation deals with the dependence of A_i and A_o on the relative numbers of binding sites on the inside and outside surfaces. Eq. (3) predicts that the ratio A_i/A_o approaches $[B]_i/[B]_o$ as the lipid concentration is lowered such that $K_1[B]_o \ll 1$ and $K_1[B]_i \ll 1$. We have reported that K_1 is in the range $(0.6-1.0)\times 10^4\ \text{M}^{-1}$. Since the number of binding sites per lipid molecule (0.25; Haynes & Staerk, 1974) is not expected to be different for the inside and outside surfaces, this ratio would be expected, in absence of electrostatic effects, to give a very close approximation to the ratios of the areas of the inside and outside surfaces. As will be shown in latter sections, the ratio is 0.63, which is close to the ratio of surface areas expected for vesicles with an outer radius of 190 Å and a membrane thickness of 40 Å.

Basic Mechanism

Since movement of the charged ANS^- implies either cotransport of a cation or countertransport of an anion, we have carried out experiments in which the ionic composition of the medium was varied. Table 1 shows how the rates ($1/t_{\frac{1}{2}}$) and amplitudes (A_i) of the reaction can be influenced to a small extent by the pH, buffer concentration and cation concentration of the medium. Lowering the pH from 7.4 to 6.1 was found to decrease the rate of permeation. This is the opposite of the expected

Table 1. Effect on buffers and pH on the $t_{\frac{1}{2}}$ for permeation of dimyristoyl PC vesicles at 35 °C

pH	Cation	[Cation]	Buffer	[Buffer]	$t_{\frac{1}{2}}$ (sec)	Amplitude[a] (arbitrary)
6.1	–	–	Imidazole	10 mM	8.0±0.0	0.32±0.02
6.1	–	–	Imidazole	100 mM	1.9±0.1	0.55±0.05
7.4	–	–	Imidazole	10 mM	5.7±1.3	0.17±0.02
7.4	–	–	Imidazole	100 mM	4.0±1.0	0.19±0.05
7.4	K^+	10 mM	Imidazole	10 mM	7.5±0.5	0.4 ±0.05
7.4	NH_4^+	8×10^{-4} M	Imidazole	10 mM	2.6±0.3	0.38±0.05
7.4	K^+	100 mM	Imidazole	10 mM	7.5±0.2	0.75±0.06
7.4	K^+ + NH_4^+	100 mM + 4×10^{-4} M	Imidazole	10 mM	2.3±0.3	0.75±0.05

[a] Volts deflection on the oscilloscope corresponding to A_i.

effect for H^+-assisted permeation, which would predict a 10-fold rate increase per unit pH decrease. It can therefore be concluded that the protonated form of ANS^- (with an estimated pK_a of 0–1) does not make significant contributions to the ANS^- permeation. Increasing the concentration of K^+ increased the reaction amplitude but not the reaction rate for $[K^+]<0.2$ M. Addition of low concentration of NH_4^+ increases the rate. The A_i values show a dependence on the ionic strength (Haynes & Staerk, 1974) which indicates that the internal cation concentration has increased to a value approaching that of the outside concentration. Experiments in which the external osmolarity was held constant at 200 mOsmolar using sucrose, gave results identical to those in which the osmolarity was not controlled.

The above result indicates that copermeation of cations is involved in the ANS^- permeation step. The mechanism of transport can be most simply described by:

$$ANS^-_{b,o} + K^+_o \underset{k_{-2}}{\overset{k_2}{\rightleftharpoons}} ANS^-_{b,i} + K^+_i \tag{4}$$

where b means membrane-bound, and o and i refer to the outside and inside surfaces, respectively. The time course of the reaction would be expected to depend on whether or not the transport reaction appreciably alters $[K^+]_i$. We shall present the results for two limiting cases.

In the first case, ANS^- binding to the inside surface results in a large enough amount of K^+ movement that the K^+ concentration inside becomes larger than that outside. In this case, $[K^+]_i=[ANS^-]_{b,i}C$, where C is a constant relating the ANS^- surface concentration to the

concentration of K^+ within the trapped volume of the vesicles. For constant $[K^+]_o$ and $[ANS^-]_o$ the integrated rate equation for the case $k_2 = k_{-2}$ becomes

$$(1-\alpha)/(1+\alpha) = \exp(-2k_2[K^+]_o t) \tag{5}$$

where

$$\alpha = A_i(t)/A_{ieq}. \tag{6}$$

This model predicts that the rate of approach to equilibrium as well as the equilibrium value will be a function of the external K^+ concentration. The equation also predicts significant deviations of the time course of advancement of the reaction from exponentiality.

In the second case, binding of ANS^- to the inside surface of the vesicle results in essentially no large perturbation of $[K^+]_i$, and one is justified in taking $[K^+]_i = [K^+]_o$. The reaction has the same overall mechanism as in Eq. (4) but the integrated rate equation becomes:

$$(1-\alpha) = \exp(-k_2[K^+]_o t). \tag{7}$$

This predicts that the reaction will have an exponential time course. Fig. 3 gives plots of the ANS^- permeation reaction according to the mechanistic assumptions of both equations. Use of Eq. (7) gives a better straight-line fit of the data. The increase in the internal K^+ concentration due to its cotransport with the ANS^- is not sufficiently large to affect the kinetics of ANS^- transport.[1]

Although Eq. (7) predicts the exponential time course of the permeation reaction, it predicts a $[K^+]_o$ dependence which is not observed experimentally. We have observed that the $t_{\frac{1}{2}}$ values for the uncatalyzed transport are independent of $[K^+]_o$ for concentrations between 3 mM and 0.2 M (*cf.* Table 1). We have tested the properties of a number of models but are not able to present one which would allow K^+ to act as a copermeant affecting reaction amplitudes but which would not predict

1 The incremental K^+ concentration within the matrix water space of the vesicle necessary to neutralize the charge of the ANS^- bound on the inside surface can be calculated using estimates of the inner and outer radii of the vesicle to calculate the inner volume and inner and outer surface areas. Such calculations show that the incremental K^+ concentration $\Delta[K^+]$ necessary for full saturation of the inside binding sites of a 500 Å diameter vesicle (50 Å thickness) with ANS^- would be 0.13 M. For a 250 Å diameter vesicle, the incremental $[K^+]$ would be 0.45 M. In the experiment of Fig. 1, with 0.1 M KCl the degree of saturation of the inner sites is about 0.19, predicting the incremental K^+ concentration of 0.025 to 0.086 M. The increment is small enough to be neglected. Smaller values of $[K^+]_o$ result in smaller degrees of ANS^- binding such that this statement is true for all the data presented in this paper.

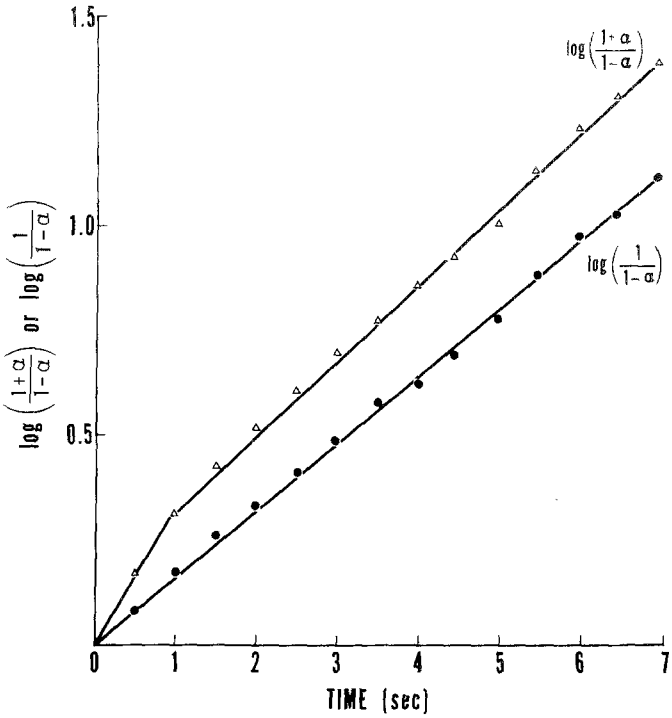

Fig. 3. Plots of the progress curve in Fig. 1 according to the assumptions of Eqs. (5) and (7)

that the $t_{\frac{1}{2}}$ for copermeation would depend on the concentration of this cation. One possible mechanism would explain the transport as the result of a transient discontinuity in the hydrocarbon chain region of the membrane such that the ANS^- and K^+ can equilibrate. The rates of uncatalyzed transport would then be dependent on the number of such "pores" and on their fractional residence time in the open state. However, observations that the half-time for monovalent cation equilibration across the membrane are several orders of magnitude longer than the $t_{\frac{1}{2}}$ values for ANS^- (and K^+) equilibration seen here (Haynes & Staerk, 1974, Papahadjopoulos & Miller, 1967) argues against the simplest version of this model. Experiments designed to measure the penetration of the first layer of multilayer vesicles gave rates identical to those of bilayer vesicles proving that the measured rates do not depend upon the radius of curvature of the membrane.

From our observations in this section, we can visualize the ANS^- permeation reaction according to the model given in Fig. 2. The net process of ANS^- permeation can be seen as the process of binding to an external binding site, transfer of the ion through the hydrocarbon chain region to a binding site on the opposite side, and dissociation of

the ANS^- from the binding site. This differs from conventional non-specific permeability mechanisms which treat the permeability as the product of the oil/water partition coefficient of the permeant and its mobility within the membrane phase. An important difference is that the present model predicts that the rate of transport will become constant at high ANS^- concentrations ($[ANS^-]_o K_1 > 1$). Another important difference is that the membrane surface is considered to be the major area of occupation whereas the conventional mechanisms assume a homogeneous distribution throughout the membrane.

An important implication of our model is that the permeation rate can be seen as the product of the degree of occupation of the membrane surface and the rate of transport across the hydrocarbon chain region. The latter will be considered as being determined by the partition coefficient of the probe between the polar head group region and the hydrocarbon chain region and by the mobility of the probe within the hydrocarbon chain region. An order of magnitude estimate of an average partition coefficient can be calculated as the ratio of the $t_{\frac{1}{2}}$ observed for permeation and that calculated using estimates of "membrane viscosity" or diffusion constants based on lateral mobility. If the diffusion constants for lateral mobility of androstan spin labels (1×10^{-8} cm^2 sec^{-1}; Träuble & Sackmann, 1972) or spin-labelled dipalmitoyl PC (1.8×10^{-8} cm^2 sec^{-1}; Devaux & McConnell, 1972) are assumed appropriate for the transverse diffusion of ANS^-, then we can calculate the root mean square time crossing the membrane from $r^2 = 2Dt$. Taking $D = 1 \times 10^{-8}$ and $r = 50$ Å we arrive at $t = 1.25 \times 10^{-5}$ sec. Taking the ratio of this calculated time to that observed (10 sec) we estimate the effective partition coefficient between the polar head group region and hydrocarbon chain region as about 10^{-6}. This corresponds to about $+4$ kcal of free energy, a value which is small when compared with the values of electrostatic free energy necessary for moving an ion from an aqueous environment to a hydrocarbon environment (Parsegian, 1969). This difference indicates either that the transient state of ANS^- transport involves ion pair formation in a low dielectric medium (*cf.* Haynes & Pressman, 1974) or that the transient state has a more polar character than the unperturbed hydrocarbon chain region.[2]

2 Tsong (1975*a*) evoked a three state model to explain changes in ANS^- permeability in the region of the crystalline to liquid-crystalline phase transition, postulating that binding in a "hydrophobic domain" could account for as much as 40% of the total ANS^- fluorescence at temperatures around the phase transition temperature T_m. Calculations of the electrostatic energy as those cited above render this interpretation unlikely. We have failed to see evidence for more than one distinct ANS^- species in fluorescent lifetime experiments conducted at T_m (Haynes & Staerk, 1974; Haynes, *unpublished observations*).

A second important implication of the model of Fig. 2 is that the binding in the polar head group region may assist in the transport of large semipolar molecules similar to ANS^-. The binding in the polar head group region would position the molecule to take advantage of random structural fluctuations in the hydrocarbon chain region which would allow penetration. Transport rates for membranes lacking polar head groups would be expected to be lower. This prediction will be tested in a later section on the effects of membrane composition.

Phase Transition Behavior

It has been shown by Chapman and co-workers (Chapman, 1965 Chapman, Byrne & Shipley, 1966; Chapman, Williams & Ladbrooke 1967; Philips, Williams & Chapman, 1969; Ladbrooke & Chapman 1969) that pure synthetic phospholipids of uniform chain length undergo sharp thermal phase transitions from the crystalline to liquid-crystalline state. We have presented evidence that these transitions involve the formation of "kinks" (Träuble & Grell, 1971; Träuble & Haynes, 1971) in the hydrocarbon chains. It is the purpose of this section to compare the effects of conformation changes on uncatalyzed and ionophore-mediated ANS^- transport. It has been shown by Tsong (*1975a, b*) that ANS^- permeability is maximum at the phase transition temperature T_m. In our experiments using vesicles which were at 35 °C until the initiation of the experiments, we found that the temperature of maximal permeability depended upon whether the temperature was scanned in the decreasing or increasing direction, as illustrated in Fig. 4. The temperature dependence of the permeability shows hysterisis in the region of the phase transition. Similar behavior was observed for a sample at 1/15th of the concentration shown in Fig. 4, indicating that if the permeability effect has its basis in aggregation of the vesicles, the aggregation must also occur at very low vesicle concentrations. The values of $1/t_{\frac{1}{2}}$ well above and below T_m are not influenced by the hysterisis. For $T<17$ °C we observed a value of 0.005 sec^{-1} and for $T=35$ °C we observed 0.1 sec^{-1} (descending curve). This is in agreement with our prediction (Träuble & Haynes, 1971) that the permeability will be higher for $T>T_m$ than $T<T_m$. Arrhenius plots of the data for high temperatures gave $\Delta H^{\ddagger}=19.2 \pm 2.0$ kcal and $\Delta H^{\ddagger}=3.1 \pm 0.1$ kcal for the increasing and decreasing temperature scans, respectively, in the 31° to 50 °C range.

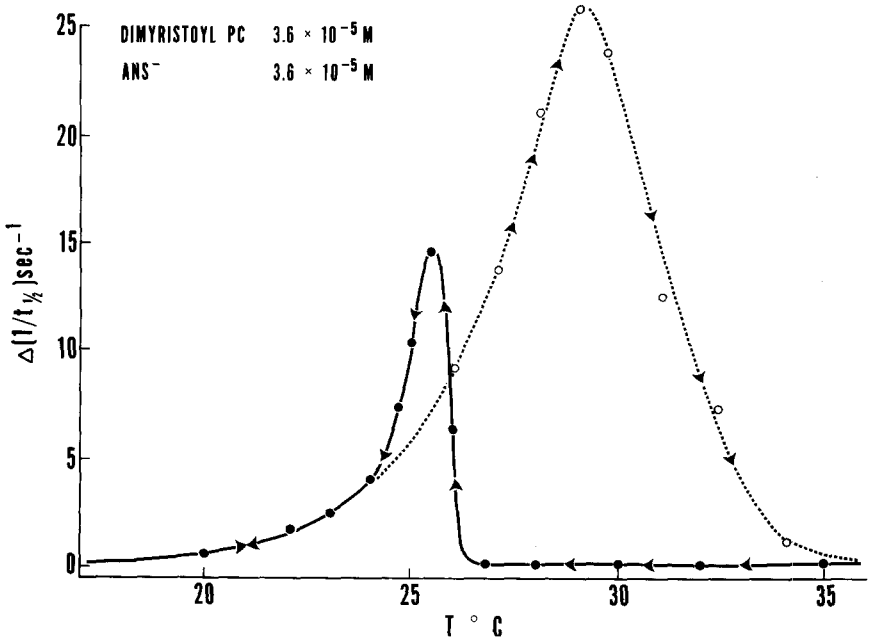

Fig. 4. The temperature dependence of ANS^- permeation for dimyristoyl PC vesicles. Syringe *A* contained vesicles (7.2×10^{-5} M dimyristoyl PC) 0.184 M KCl and 2 mM tris buffer, pH approx. 7.4. Syringe *B* contained 1.32×10^{-4} M ANS^-. The vesicles were prepared and stored at 35 °C and had no exposure to a lower temperature before initiating the experiment. The temperature of the reactants was varied in the direction indicated by the arrows, and the stopped-flow experiment was carried out. The average temperature scan speed was approx. 0.3 deg/min. In the case of the increasing temperature scan, fresh reactants were brought very rapidly to 4 °C and the experiment was initiated. When the experiment was carried out by bringing the reactants from 30 °C directly to the temperature of study, results intermediate between those of the two curves were obtained

Fig. 5 shows that the effect of the phase transition is less pronounced for the case of valinomycin-catalyzed ANS^- permeation. A shoulder is found at approximately 23 °C. The rates at 35 °C and higher are due to valinomycin-induced catalysis and are much larger. We interpret this to mean that valinomycin can make use of the postulated disorder in the interfaces of regions consisting of extended and "kinked" chains to accomplish transport in the region of the phase transition, but that for full expression of the transport-inducing capabilities of the molecule, a high degree of chain disorder is necessary. Arrhenius plots of the high temperature region of the curve $\Delta H^{\ddagger} = 16.3 \pm 0.5$ kcal for valinomycin-assisted ANS^- transport. In contrast, the uncatalyzed ANS^- permeation is most effective when faults are present in the packing of the hydrocarbon chain region. This is what would be expected if uncatalyzed

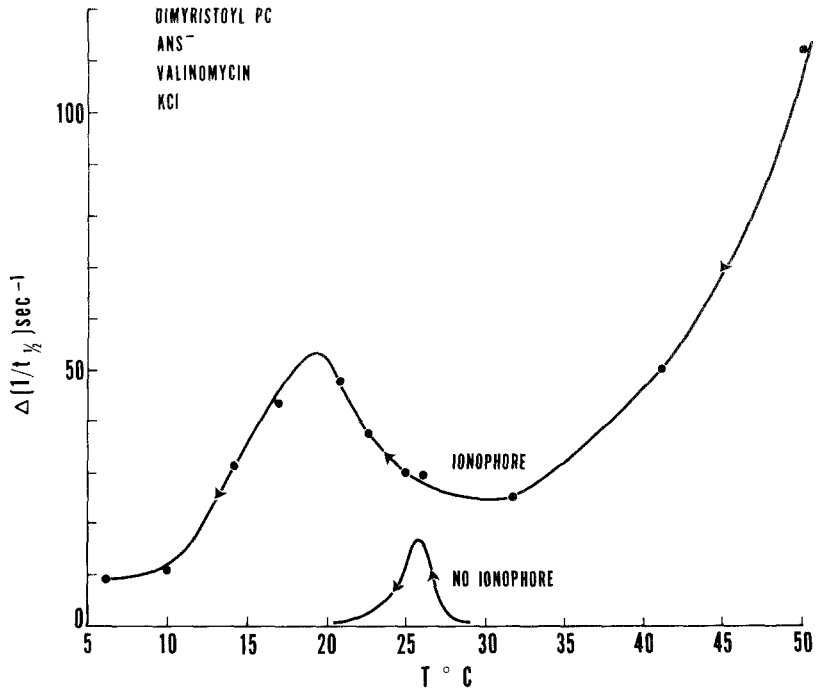

Fig. 5. The temperature dependence of the valinomycin-catalyzed transport rate for dimyristoyl PC vesicles. The lower curve gives the behavior in absence of ionophore. Syringe *A* contained 2.1×10^{-4} M dimyristoyl PC vesicles, 6.7×10^{-6} M valinomycin, 0.184 M KCl and 2 mM tris, pH 7.4. Syringe *B* contained 1.92×10^{-5} M ANS^-. The temperature scan speed was approx. 3 min/deg

permeation depends upon "transient pores" and if ionophore-catalyzed permeation depends upon "hydrocarbon chain mobility".

We have attempted to determine whether aggregation parallels the temperature dependence of ANS^- permeability by carrying out light scattering experiments. Yi and MacDonald (1973) have studied changes in the turbidity and light scattering of dipalmitoyl PC dispersions and compared them with refractive index increments (dn/dc) and partial volumes (dV/dc) measured in the same system. They showed that there were large light scattering changes and hysteresis effects in the "pre-transition" region 7–10° below the phase transition temperature (T_m). Their analysis indicated that these effects were larger than could be accounted for changes in dn/dc or dV/dc with temperature and they attributed them to an aggregation-disaggregation process. Fig. 6 gives evidence for temperature-dependent aggregation changes in our uni-lamellar preparation of dimyristoyl PC. Vesicles prepared at 35 °C and

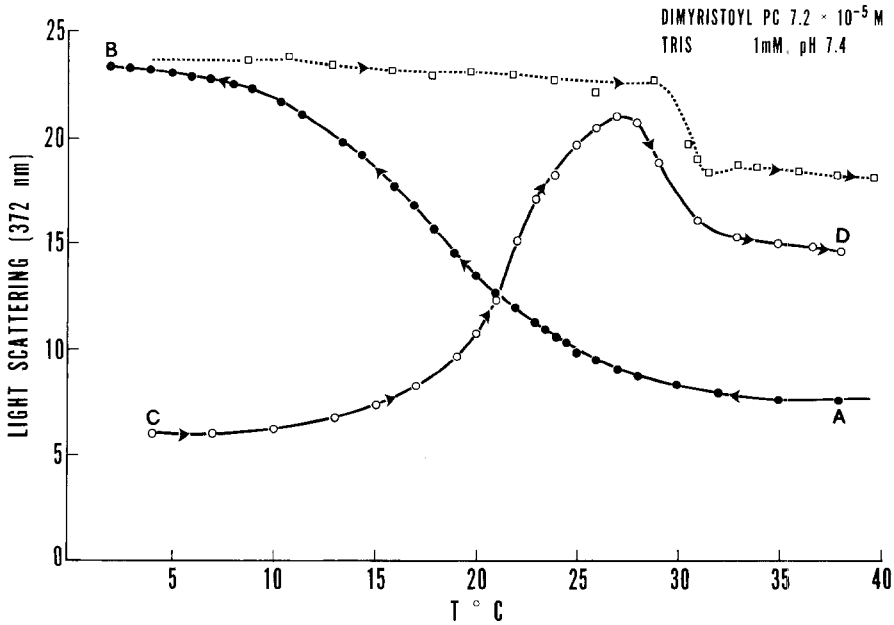

Fig. 6. The temperature dependence of light scattering of a suspension of dimyristoyl PC vesicles. Light scattering of a 7.2×10^{-5} M dimyristoyl PC suspension in 1 mM tris buffer, pH approx. 7.4, was monitored at 372 nm in the fluorometer. The temperature scan speed was approx. 0.3 deg/min

stored at this temperature give low levels of light scattering (State *A*). Descending slowly in temperature causes ca. two fold increase in light scattering which shows up as a broad transition centered at ca. 18 °C. The major portion of this change is due to changes in aggregation or vesicle size, since the light scattering in State *B* is much larger than that in State *C*. In the latter state the vesicles stored at 35 °C have been brought very rapidly from 35 to 4 °C. Ascending in temperature from State *C* produces an increase in light scattering centered at ca. 22 °C, followed by a decrease to the level of State *D* intermediate between that of *A* and *B*. Scanning to lower temperatures produces a sharper and more reversible transition between State *D* and State *B*. For the interpretation of these results, it is necessary to recognize that for a given temperature, dn/dc and dV/dc will be constant, so that the vertical distance between the curves will indicate differences weight-average "molecular weight" of the aggregate. The above indicates that the vesicles undergo time-dependent and irreversible aggregation and/or fusion in the region of the phase transition temperature. It also suggests that the permeability peak in the phase transition region may involve

effects of aggregation. Further experiments were carried out to test this conclusion.

Addition of 1 mM $LaCl_3$ to dimyristoyl lecithin vesicles reduced the temperature sensitivity of the ANS^- permeation rate in the temperature range 13–41 °C. All the $t_{\frac{1}{2}}$ values fell in the range 4–9 sec and the permeability peak at 23 °C was destroyed. In experiments analogous to that of Fig. 6, the light scattering was found to be temperature-insensitive, showing less than 10% variation over the temperature range 13–41 °C. It is uncertain whether La^{3+} destroys the phase transition, but our previous studies have shown that the cation binds to dimyristoyl PC vesicles, imparting them with a net positive charge (Haynes, 1974). Electrostatic repulsion between the vesicles must be responsible for the decreased temperature-dependent aggregation observed in the presence of La^{3+}.

Since the above results do not prove whether it is the phase transition or the aggregated state which is responsible for the increase in the rate of "uncatalyzed" ANS^- permeation, we have investigated ANS^- transport in vesicles which can be brought into the aggregated state without manipulating the temperature and phase transition. Addition of divalent cations to vesicles containing dimyristoyl PC and a large mole fraction of PA^- (derived from egg PC) results in aggregation of the vesicles (Lansman & Haynes, 1975). The degree of aggregation has a high power dependence on the mole fraction of PA^-. Table 2 shows that Ca^{2+} addition to 5:5 PC/PA vesicles increases the rate of the two permeation processes found in these vesicles. Under these conditions, it is estimated

Table 2. Effect of Ca^{2+}-induced aggregation on ANS^- permeation with dimyristoyl PC/PA 5:5 vesicles at 35 °C

Final composition at (mM)	Reaction 1		Reaction 2		
	$t_{\frac{1}{2}}$ (sec)	A_i	$t_{\frac{1}{2}}$ (sec)	A_i	A_o
1 KCl	27	0.016	325	0.016	0.126
1 KCl, 2.5 $CaCl_2$	1.4	0.027	–	–	0.74
100 KCl	2.6	0.015	120	0.043	0.44
100 KCl, 2.5 $CaCl_2$	0.85	0.020	125	0.040	0.59
100 KCl, 8.8 $CaCl_2$	1.2	0.016	6	0.044	0.84

Obtained from stopped-flow experiments of the format of Table 1. The first solution contained 1 mM tris buffer, pH 7.4. Two kinetically-separable reactions were observed.

that at least 4% of the vesicles are in the aggregated state. It is impossible to carry out this experiment in the totally aggregated state with pure PA vesicles because the latter do not bind ANS^-. The analysis of the kinetics of the aggregation process (Lansman & Haynes, 1975) implies a rapid interconversion of aggregated and nonaggregated vesicles with a $t_{\frac{1}{2}}$ of ca. 0.5 sec for the process. The Ca^{2+} effect on ANS^- permeation is absent in 8:2 PC/PA and pure PC vesicles which show no detectible aggregation. Thus in all the systems studied it was found that aggregation is accompanied by an increase in "uncatalyzed" transport of ANS^- and that this effect was not observed when aggregation could not occur. This raises the question of whether the aggregation, fusion (Papahadjopoulos *et al.*, 1974) and permeation reactions all depend upon the same disorder structures in the hydrocarbon chain region.

Effects of Lipid Composition on the Permeation Rate

Table 3 gives information on the effect of lipid composition on the $(1/t_{\frac{1}{2}})$ values and rates of ANS^- transport in the absence and presence of valinomycin. The experimental quantity $1/t_{\frac{1}{2}}$ is the measure of the rate of transfer of ANS^- to an internal binding site from an external one, while the overall transport rate will be given as $(1/t_{\frac{1}{2}}) \times A_i$. In the uncatalyzed case, the overall transport rate decreases with the inclusion of cholesterol, phosphatidic acid (PA^-) and phosphatidyl ethanolamine (PE) in

Table 3. Effects of lipid composition on the rates of ANS^- permeation[a]

Composition	$(1/t_{\frac{1}{2}})_{normal}$ (sec^{-1})	$(1/t_{\frac{1}{2}}) \times A_i$ (sec^{-1})	$(1/t_{\frac{1}{2}})_{val}$ (sec^{-1})	$(1/t_{\frac{1}{2}}) \times A_i$ (sec^{-1})	$(1/t_{\frac{1}{2}})_{val}/(1/t_{\frac{1}{2}})_{normal}$
Dimyristoyl PC	0.12	0.12	66	66	550
Dimyristoyl PC/PE 8:2	0.005 – 0.02	0.0035 – 0.014	100	70	5000 – 20,000
	2.4[b]	1.7[b]	100[b]	70[b]	41[b]
Dimyristoyl PC/cholesterol 2:1	0.26	0.057	50	11	192
Dimyristoyl PC/PA 8:2	0.10	0.044	17	7.5	170

[a] The experiments were carried out at 35 °C in the following configuration: Syringe $A - 1 \times 10^{-4}$ M lipid, $\pm 3 \times 10^{-6}$ M valinomycin, 0.9 M KCl and 1 mM tris buffer, pH 7.4; Syringe $B - 1.9 \times 10^{-4}$ M ANS^-, and 1 mM tris buffer, pH 7.4. The values of A_i are normalized to those of dimyristoyl PC. The uncertainty in the ratios given in the last column is ca. 30%.

[b] For vesicles stored at low temperature and returned to 35 °C for measurement.

the dimyristoyl PC membrane. Previous studies (Haynes & Staerk, 1974) showed that the number of ANS^- binding sites in these mixtures ($[B]_{mix}$) is smaller than in pure PC membranes, $[B]_{PC}$. The relationship between $[B]_{mix}$ and $[B]_{PC}$ is given approximately as

$$[B]_{mix} = [B]_{PC} \times f_{PC}{}^4 \tag{8}$$

when f_{PC} is the mole fraction of PC on the lipid mixtures.

Table 3 shows that the $1/t_{\frac{1}{2}}$ values are not affected by the lipid substitution as much as the A_i values. Therefore, we consider the decrease in permeability to be primarily the effect of the lipid substitution on the number of ANS^- binding sites on the membrane surface. The contribution of pathway II of Fig. 2 must be small.

In contrast, the incorporation of dimyristoyl PE and incubation at low temperatures renders values of $1/t_{\frac{1}{2}}$ and $(1/t_{\frac{1}{2}}) \times A_i$ higher than for PC despite the fact that A_i has been reduced by the PE incorporation. It should be noted that the PE probably engaged in head-to-tail hydrogen bonding with itself and the PC (Haynes & Staerk, 1974) and that these polar head group interactions may increase the probability of formation of the transient in the permeability mechanism. Repetition of the experiment described above at pH 10.5 where the amino group is not ionized and the vesicles carry a net negative charge gave $1/t_{\frac{1}{2}}$ values which were characteristic of pure PC. The effect of temperature on PC/PE mixtures will be discussed in the next section.

Incorporation of cholesterol or PA into the PC membrane also reduces the rate of valinomycin-catalyzed ANS^- transport. The cholesterol effect can be explained either in terms of changes in surface structure nonconducive to valinomycin-K^+ complex formation or a decrease in membrane "fluidity", while the PA^- effect is probably an effect of the absence of the polar head group on the action of the ionophore.

The final column of Table 3 gives the ratios of the rates obtained in the presence and absence of valinomycin. In terms of the hypotheses of the previous section, this can be considered as the quotient of the effect of the change of the lipid on the efficacy of carrier-mediated transport to that of transport relying on "transient pore" structures.

Effect of Temperature on Mixed Membranes

Incorporation of 33 mole percent cholesterol in the membrane destroys the phase transition and destroys the permeability peak in the

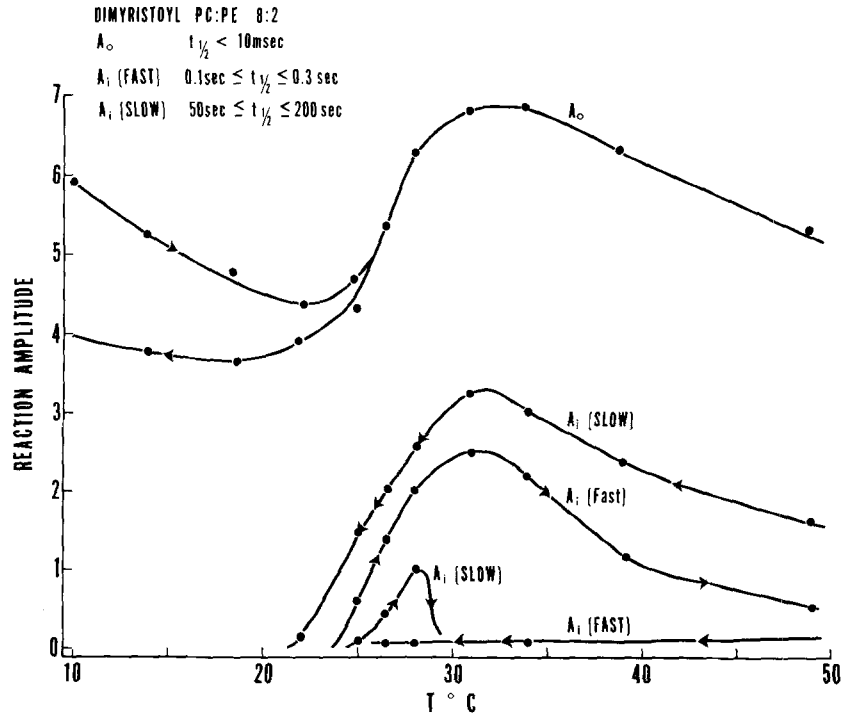

Fig. 7. Temperature dependence of the amplitudes of the fast and slow reactions of dimyristoyl PC/PE, 8:2 vesicles. Reaction conditions: 3.5×10^{-5} M total lipid, 9.6×10^{-5} M ANS, 0.094 M KCl, 1 mM tris buffer, pH approx. 7.4. The temperature scan speed was approx. 0.3 deg/min. The ascending scan was made on a sample that was brought directly from the temperature of storage (50 °C) to 10 °C

region of 26 °C. This is in accordance with our observation that cholesterol and lecithin are well mixed above and below the phase transition temperature, as deduced from analysis of equilibrium experiments on the binding site with high quantum yield (Haynes & Staerk, 1974; Haynes, *unpublished*). A similar conclusion has been arrived at by Tsong (1975*b*) on the basis of kinetic data for 20 mole percent cholesterol dimyristoyl PC mixture. Arrhenius plots of the present rate data for high temperatures gave $\Delta H^{\ddagger} = 16.7 \pm 0.3$ for uncatalyzed transport.

Incorporation of dimyristoyl PE into membranes of dimyristoyl PC also destroys the permeability peak at the $T_{m(PC)}$ and produces hysteresis effects in the temperature-dependence of the permeability. For vesicles prepared and stored at temperatures above $T_{m(PC)}$, the effect of the PE addition is to increase the $t_{\frac{1}{2}}$ value from 10 sec to 500 – 200 sec. Fig. 7 compares the effect of scanning downwards with the effect of scanning upwards on the temperature dependence of the amplitudes of binding on

the outside (A_o) and inside (A_i) surfaces. The temperatures of the experiment were below the T_m of the PE. In addition to the slow process, there is evidence for a fast process of extremely small amplitude ($A_i/A_o = 0.02$). This may represent the permeation of ANS^- through a small atypical fraction of the vesicles or may indicate a slow ANS^--induced structural transition within all of the vesicles. Descending in temperature causes both this process and the slow permeation process to disappear.

When a sample is brought down quickly from its storage temperature to 10 °C and is scanned in the direction of increasing temperature, the amplitude of the fast process is increased at the expense of the slow one. This suggests that incubation of the mixed vesicles below T_m induces a structural change which is not easily reversed at temperatures above T_m. The structural change might be inter-membrane aggregation or fusion occurring as the result of formation of separate PE phases for $T < T_{m(PC)}$.

Catalysis of Transport by Ionophores

Acceleration of the rate of ANS^- transport across bilayer membranes in the presence of valinomycin and K^+ has been reported by Gains and Dawson (1975). In this section, we extend this observation to 35 neutral ionophore and cation combinations and we will discuss the mechanism by which neutral ionophores catalyze ANS^- transport. A carrier mechanism is indicated since the effect is dependent on alkali cations, being absent when only Ca^{2+} is present. Furthermore, the effect shows a K^+/Na^+ specificity, attributable to ionophorous action; uncatalyzed permeation shows no discrimination among the alkali cations (with the exception of >0.5 M LiCl). In order to quantitate the catalytic effect of the ionophores we have used the incremental rate of permeation, $\Delta(1/t_{\frac{1}{2}})$

$$\Delta(1/t_{\frac{1}{2}}) = (1/t_{\frac{1}{2}})_{\text{ionophore}} - (1/t_{\frac{1}{2}})_{\text{no ionophore}}. \tag{9}$$

The value of $\Delta(1/t_{\frac{1}{2}})$ behaves as expected for carrier-mediated transport. It is proportional to the ionophore concentration for phospholipid to ionophore ratios greater than 15. The value of $\Delta(1/t_{\frac{1}{2}})$ increases with increasing concentrations of monovalent cations (M^+ as shown in Fig. 8). The latter example is in direct contrast to the case of uncatalyzed permeation which shows little dependence of $1/t_{\frac{1}{2}}$ on $[M^+]$. The above constitutes excellent evidence that the ionophores are behaving as carriers for ANS^-. We propose the following scheme as the minimal mechanism of ANS^- transport consistent with the data.

$$M_o^+ + I_{b,o} \underset{k_{-2}}{\overset{k_2}{\rightleftharpoons}} M^+ - I_{b,o} \tag{10}$$

(complexation of the outside surface)

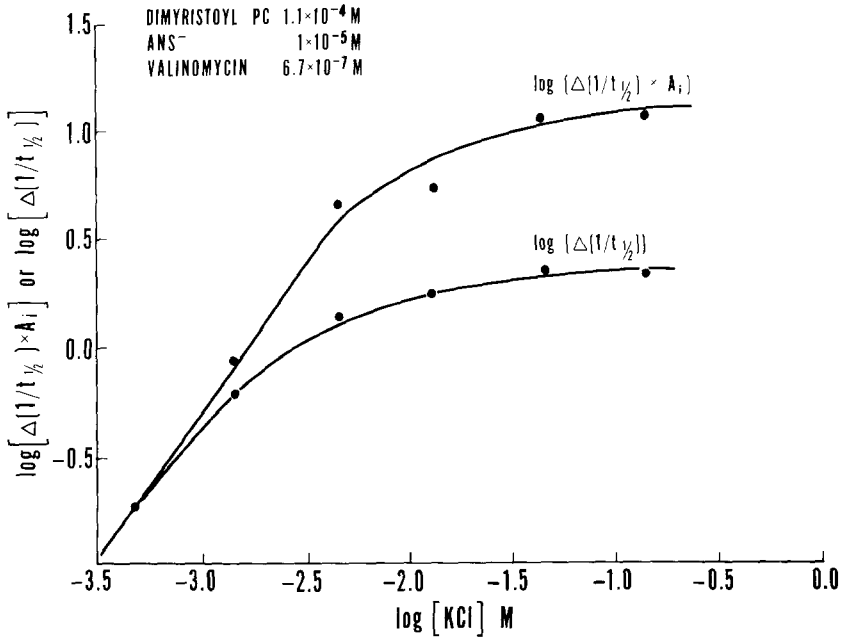

Fig. 8. The $[K^+]$ dependence of valinomycin-facilitated ANS^- transport at 35 °C. Syringe *A* contained 1.34×10^{-6} M valinomycin, 2.2×10^{-4} M dimyristoyl PC, 5 mM histidine buffer, pH 7.4 and a variable $[K^+]$. Syringe *B* contained 5 mM histidine buffer, pH 7.4 and 2×10^{-5} M ANS^-

$$M^+ - I_{b,o} + \mathrm{ANS}_o^- \underset{k_{-3}}{\overset{k_3}{\rightleftharpoons}} M^+ - I_{b,i} + \mathrm{ANS}_{b,i}^- \tag{11}$$

(cotransport)

$$I_{b,i} \underset{k_{-4}}{\overset{k_4}{\rightleftharpoons}} I_{b,o} \tag{12}$$

(return of uncomplexed ionophore).

The symbol I represents the ionophore, b denotes membrane-bound species, and i and o represent the inside and outside membrane surface. It is possible that the process of Eq. (11) is more complicated than indicated, occurring by the mechanism of ion pairing:

$$M^+ - I_{b,o} + \mathrm{ANS}_o^- \underset{k_{-3a}}{\overset{k_{3a}}{\rightleftharpoons}} (M^+ - I - \mathrm{ANS}^-)_{b,o} \tag{13}$$

with transport of the ion pair

$$(M^+ - I - \mathrm{ANS}^-)_{b,o} \underset{k_{-3b}}{\overset{k_{3b}}{\rightleftharpoons}} (M^+ - I - \mathrm{ANS}^-)_{b,i} \tag{14}$$

and with the process analogous to that of Eq. (13) occurring also on the inside surface to complete the cycle.

Table 4. Efficacy of ionophore-cation combinations for ANS^- transport

Ionophore	$\Delta(1/t_{\frac{1}{2}})/[I](\times 10^{-6})\,M^{-1}\,sec^{-1}$ for:				
	Cs^+	Rb^+	K^+	Na^+	NH_4^+
Valinomycin	1.31	1.73	2.60	0.26	1.25
Nonactin	0.82	1.01	1.57	0.53	5.99
Monactin	1.34	2.55	3.03	1.25	16.9
Dinactin	1.07	2.40	4.21	0.87	25.2
Trinactin	0.76	2.79	6.50	0.45	31.1
Enniatin B	0.212	0.322	0.632	0.132	0.195
18-crown-6	0.0277	0.196	0.510	0.0517	0.168

The experiments were carried out with 0.1 M MCl (or 0.05 M NH_4Cl), 1.4×10^{-4} M dimyristoyl-L-phosphatidyl choline, 3×10^{-5} M ANS^-, 1 mM tris, pH 7.6 at 33 °C. The experiments were conducted using the following ionophore concentrations: valinomycin, 7×10^{-7} M; macrolide actins, 2×10^{-6} M; enniatin B, 1.2×10^{-5} M; 18-crown-6, 4.21×10^{-5} M. $\Delta(1/t_{\frac{1}{2}})$ was taken as the difference in $1/t_{\frac{1}{2}}$ in presence and absence of the ionophore. The amplitude to the fluorescence change was influenced significantly by the choice of cation or by the ionophore at the concentrations used.

Table 4 shows the ion and ionophore specificity for catalyzed transport for the cases tested. We will make some preliminary observations from these data before considering the mechanism of cotransport in greater detail in the next section. The dynamic range covered in Table 4 is only a factor of 1000 and the ion and ionophore specificities are quite low compared with the results of other model and biological membrane systems tested (Haynes & Pressman, 1974; Haynes, Wiens & Pressman, 1974). Thus monactin shows a K^+/Cs^+ specificity of 2.3 in the vesicle system, whereas the value for mitochondrial transport is 9. Similarly, in the mitochondrial system, the relative efficacy of valinomycin, monactin, enniatin B and 18-crown-6 for K^+ transport is 1.0, 0.62, 0.0022, 0.000044, while the corresponding relative efficiencies for K^+-facilitated ANS^- transport are 1.0, 1.16, 0.242 and 0.195. However, the rank order of efficacy between the different groups of ionophores and the rank order between the members of the macrolide actin series (monactin through trinactin) are retained. Furthermore, the rank order of cation selectivity of all of the ionophores is retained with $K^+ > Rb^+ > Cs^+ > Na^+$, and the macrolide actins show their inherent NH_4^+/K^+ specificity. We are thus dealing with a carrier-function-related property, although it is one which seems to have been modified by the necessity for cotransport of ANS^-.

Electrically-Coupled Cotransport vs. Ion Pair Model

It is important to our consideration of the ion specificity data of Table 4 to have a more precise description of the mechanism by which the ionophores assist ANS$^-$ transport. To begin with, we note that models which assume that the membrane behaves as a bulk oil phase and "extracts" equal amounts of $I-M^+$ and ANS$^-$ as free ionic species (Ciani, Eisenman & Szabo, 1969; Eisenman, Ciani & Szabo, 1969; Szabo, Eisenman & Ciani, 1969; Haynes & Pressman, 1974; Haynes *et al.*, 1974), are inappropriate because they predict $[M^+]^{\frac{1}{2}}$ and $[\text{ANS}^-]^{\frac{1}{2}}$ dependencies of ANS$^-$ transport, whereas first power dependencies are observed. We are left with two cases: (*a*) Electrical neutrality *within* the membrane is not observed, and ANS$^-$ copermeates with $I-M^+$ as a free, albeit electrically-coupled species (Eq. (11)), or (*b*) ANS$^-$ permeates in an obligatory fashion as an $I-M^+$-ANS$^-$ ternary complex (Eqs. (13) and (14)). In case (*a*), the ion specificity would be low because the ANS$^-$ permeability would constitute a rate limitation, such that the intrinsic ion and ionophore specificities would be degraded to the same low level. In case (*b*), the ion specificities of the overall transport reaction would be a function of the equilibrium constant for formation of the ternary $I-M^+$-ANS$^-$ complex as well for the formation of $I-M^+$ complex. Case (*b*) is favored, and it will be described in greater detail in the next section. The remainder of this section will be used to describe an experiment which excludes case (*a*) and shows that electrogenic effects of $I-M^+$ do not appreciably affect the rate of ANS$^-$ transport.

The electrically-coupled cotransport model would predict that the ionophores establish rapidly a diffusion potential to which the ANS$^-$ transport responds. ANS$^-$ transport would be considered to be the rate-limiting step in the reaction sequence, with the rate of transport responding directly to the membrane potential set up by the ionophore and cation gradient. An experiment was devised to test this possibility. Vesicles were preincubated with valinomycin and were then subjected to varying KCl concentrations such that the KCl concentration inside the vesicle was either (*a*) twice as large as the final concentration of KCl after rapid mixing, (*b*) was equal to the final KCl concentration after mixing or (*c*) was 1 mM. If it is assumed that an electrophoretic K^+ permeability induced by valinomycin is the primary ionic permeability in the system, then the membrane potential, V_m, would be given by

$$V_m=(RT/F)\ln([K^+]_o/[K^+]_i) \tag{15}$$

where $[K^+]_o$ and $[K^+]_i$ are the external and internal K^+ concentrations, respectively. Recent work of Läuger and co-workers (Ketterer, Neumcke & Läuger, 1971) has shown that the conductance of lipophilic ions in black lipid membranes is a function of V_m and that this dependence is expressed as an $\exp(eV_m/2kT)$ dependence of the rate constant for the trans-membrane step of the charge-transporting reaction. For our intended consideration of the V_m dependence of the ANS^- transport reaction we would expect

$$\Delta(1/t_{\frac{1}{2}}) = k_o \exp(eV_m/2kT) \tag{16}$$

where k_o is a proportionality constant equal to $\Delta(1/t_{\frac{1}{2}})$ for $V_m = 0$. Combination of Eqs. (15) and (16) gives

$$\Delta(1/t_{\frac{1}{2}}) = k_o([K^+]_o/[K^+]_i)^{\frac{1}{2}} \tag{17}$$

predicting that the ANS^- transport rate will have a 1/2 power dependence on the K^+ concentration ratio. The values of the latter in the experiment above are 0.5, 1.0, and 100. The corresponding values of $\Delta(1/t_{\frac{1}{2}})/k_o$ will be 0.71, 1.0 and 10. However, it was observed experimentally that $\Delta(1/t_{\frac{1}{2}})$ was not affected by the changes of K^+ concentration in this experiment. Although the calculated values could be much closer to 1.0 due to perturbations of $[K^+]_i$ during the course of the rapid mixing experiment, we consider the above result to show that $[ANS^-]$ is not responding electrophoretically to a valinomycin-K^+-induced V_m. It must therefore be concluded that either the concentration ratios established under these circumstances do not affect the rate of ANS^- transport or that the gradients are discharged in less than 30 msec of the time of their establishment. The second interpretation implies an initial turnover of ca. 300 per sec for valinomycin transporting KCl and it also implies that Cl^- crosses more rapidly than ANS^-. Although this seems unlikely for reasons of charge delocalization and our observations about relative extractability of these two anions into organic phases (Haynes & Pressman, 1974), an additional experiment was carried out to test this possibility. It was found that the $t_{\frac{1}{2}}$ for ANS^- permeation for case (*c*) was independent of whether K^+ was supplied as the Cl^- salt or as the $SO_4^=$ salt. The divalent anion is not expected to permeate, and the lack of an effect of Cl^- on ANS^- permeability indicates that ANS^- is the most permeant anion in the system. This negates the second interpretation described above and we are left to conclude that membrane potentials do not contribute to the rate observed by our technique and that ANS^- must be transported primarily as a ternary $I-M^+$-ANS^- complex.

This conclusion is at variance with the conclusion of Bakker and van Dam (1974) that ANS^- fluorescence responds to K^+ "diffusion potentials" in phospholipid vesicles through transient fluorescent changes obtained upon the addition of valinomycin. Although we differ with them in interpretation, a close consideration shows no discrepancy between their experimental results and ours. In their studies, fluorescence increases were obtained for inwardly-directed K^+ gradients and decreases were obtained for outwardly-directed K^+ gradients. Three observations were crucial to a more exact interpretation of their experiments: (*a*) The effect of valinomycin addition was transient, and was followed by a slower reversal in the direction approaching the value obtained prior to the valinomycin addition. (*b*) The effect was observed under conditions in which the ANS^- was incompletely pre-equilibrated across the membrane (present authors' interpretation). (*c*) The effect was observed with soybean phospholipids bearing negative charge but was not observed with egg lecithin membranes bearing no charge. This last observation shows that there exists no discrepancy in terms of experimental results. These observations suggest that the effect has as its basis a coupled transport of K^+ and ANS^- and that the "overshoot" is a consequence of dependence of ANS^- binding on membrane surface potential. The following explanation is sufficient to account for the result. With the negatively-charged membranes, the degree of ANS^- binding is low, and the tight coupling of ANS^- transport with K^+ transport results in an outwardly-directed ANS^- gradient. The amplitude of the transient would be determined by the final value of $[ANS^-]_i$ and its binding constant for the inside surface. The slow reversal of the change would be the result of a slower dissipation of the ANS^- gradient by Cl^- for ANS^- exchange catalyzed by the ionophore. The effect is seen as the result of changes in the degree of ANS^- binding, although direct effects of membrane on the probe's quantum yield can also contribute. Table 5 contrasts the behavior of ANS^- in the present study with that expected for a membrane potential probe which responds directly and instantaneously to a valinomycin-induced K^+ diffusion potential. The comparison shows that ANS^- does not act as a membrane potential probe in our system. This is in contrast to the behavior of the cationic cyanine dyes (Sims *et al.*, 1974) whose binding and trans-membrane distribution do respond to K^+ diffusion potentials induced by valinomycin. An important difference between these dyes and ANS^- lies in their charge and the inability of the cationic dyes to ion pair with a valinomycin-K^+ complex.

Table 5. Comparison of predictions of the diffusion potential and cotransport models with the observed behavior in ionophore experiments

	Effect for diffusion potential model	*Effect for cotransport* model	*Observed effect in* present study
Time dependence of the fluorescence change	The fluorescence change should be instantaneous and should remain at a constant value. When the K^+ gradient is discharged the effect should be reversed	The fluorescence should increase as a function of time and approach a limiting time-independent value	The fluorescence increase as a function of time and approaches a limiting time-independent value
Effect of increasing the ionophore concentration	The fluorescence increase should be independent of *ionophore concentration over* a large range	The rate, but not the magnitude, of the fluores*cence increase should* increase with increasing ionophore concentration	The rate but not the magnitude of the fluorescence increase *increases with increasing* ionophore concentration
Effect of increasing $[K^+]$ out	Instantaneous increase in fluorescence	An increase in both the magnitude and the rate of the fluorescence increase	An increase in both the magnitude and the rate of the fluorescence increase
Effect of increasing [lipid] at low $[ANS^-]$	No effect	The relative amplitude of the fluorescence increase diminishes, tending toward zero	The amplitude of the fluorescence increase diminishes, tending toward zero
Effect of increasing $[ANS^-]$ at low [lipid]	No effect on relative amplitude	Increase in amplitude. Increase in rate of fluorescence increase	Increase in amplitude. Increase in rate of fluorescence increase

Detailed Mechanism Involving Ion Pairing

Experiments were carried out to determine the M^+ concentration dependence of ionophore-facilitated ANS$^-$ translocation and to estimate the equilibrium constants for $I-M^+$ formation (K_2) and $I-M^+$-ANS$^-$ formation (K_3—the equilibrium constant for the process of Eq. (13)) and the rate constants for ionophore or ternary complex translocation (k_{3b} or k_4). We have assumed that the translocation of the ternary complex is an obligatory and rate-limiting step of the overall reaction, such that

$$d[\text{ANS}^-]_{b,i}/dt = k_{3b} \quad [I-M^+\text{-ANS}^-]_{b,o}. \tag{18}$$

Blok, de Gier and Van Deenen (1974) have given evidence for a similar mechanism for valinomycin-facilitated K^+ (CNS^-) efflux from liposomes. It is further assumed that the interfacial complexation and decomplexation steps are rapid, such that $k_{-2} > k_4 > k_{3b}$. The following expression can be derived for the dependence of the transport rate on $[M^+]_o$ and $[\text{ANS}^-]_o$:

$$d[ANS^-]_i/dt = \frac{k_{3b}[I]_t K_2 K_3 [M^+]_o [\text{ANS}^-]_o}{1+K_2[M^+](1+K_3[\text{ANS}^-]_o)}. \tag{19}$$

This equation predicts saturation properties with regard to both $[M^+]_o$ and $[\text{ANS}^-]_o$ with the apparent binding constant for M^+ given as:

$$K_{\text{app}(M^+)} = K_2(1+K_3[\text{ANS}^-]_o) \tag{20}$$

and with the apparent binding constant for ANS_o^- given as:

$$K_{\text{app}(\text{ANS}^-)_o} = \frac{K_2 K_3 [M^+]_o}{1+K_2[M^+]_o}. \tag{21}$$

For low ANS$^-$ concentrations ($K_3[\text{ANS}^-]_o \ll 1$), we have $K_{\text{app}(M)^+} = K_2$ and the correct value of K_2 is given as the reciprocal M^+ concentration for half-maximal translocation rate. Fig. 8 shows the dependence of $\Delta(1/t_{\frac{1}{2}}) \times A_i$, a quantity proportional to $d[\text{ANS}^-]_{b,i}/dt$, on the external K^+ concentration. Values of $\Delta(1/t_{\frac{1}{2}})$ are plotted for comparison. Log-log plots of these quantities were linear for low concentrations, but leveled off at high concentrations. The initial slopes for $(1/t_{\frac{1}{2}}) \times A_i$ and $(1/t_{\frac{1}{2}})$ are 1.4 and 1.2, respectively. The values are significantly higher than 1.0, the theoretical value for 1:1 complexation in absence of electrostatic surface potential effects. Higher values could be accounted for by the effect of the positive charge of the complexes on the membrane surface to increase the degree of ANS$^-$ binding and ion pairing. The rates tend to saturate

at higher $[K^+]_o$ values. Double reciprocal plots gave a K_2 value of $15 M^{-1}$ based on $(\Delta(1/t_{\frac{1}{2}}) \times A_i)$. A similar experiment carried out with dimyristoyl PC/PA 8:2 vesicles gave a slope of 0.84 and gave a K_2 value of $5 M^{-1}$. These values can be taken as the apparent association constants for Val-K^+ on these membranes at the membrane surface potential and $[ANS^-]_o$ values of the study.

The rate data for K^+ and Na^+ transport facilitated by valinomycin, monactin, enniatin B and 18-crown-6 were analyzed according to the model of Eq. (19). The values of K_2 were determined from double reciprocal plots of the transport rate $(\Delta 1/t_{\frac{1}{2}} \times A_i)$ against $[M^+]_o$ for low $[ANS^-]_o$ (Eq. (20)). The values of K_3 were calculated from Eq. (21) using the K_2 value and the $K_{app(ANS^-)}$ value determined from double reciprocal plots of the rate against $[ANS^-]_o$ with 0.1 M MCl. The value of k_{3b} was then determined from the intercept of the latter plot. Values of K_2, K_3 and k_{3b} for K^+ and Na^+ with the four ionophores are given in Table 6.

We note that for valinomycin and monactin the K^+ complexation constants are larger than the Na^+ complexation constants. However, the K^+/Na^+ specificity of K_2 for monactin is much smaller than for two phase extraction (Haynes & Pressman, 1974) and for transport through the mitochondrial membrane (Haynes *et al.*, 1974). The K^+/Na^+ specificity of K_2 for enniatin B is indeterminate and that for 18-crown-6 is reversed. In the latter case we are dealing with an ionophore with appreciable solubility and complexing ability in the aqueous phase

Table 6. Complexation constants and maximal turnover number at 35 °C

Ionophore	Cation	K_2 M^{-1}	K_3 M^{-1}	k_{3b} sec^{-1}
Valinomycin	K^+	14	1.5×10^4	46
Valinomycin	Na^+	$\leqq 0.5$	$\geqq 3.3 \times 10^5$	26
Monactin	K^+	14	2.4×10^3	122
Monactin	Na^+	2.3	4.8×10^4	16
Enniatin B	K^+	$\leqq 0.7$	$\geqq 2.4 \times 10^5$	4.8
Enniatin B	Na^+	$\leqq 0.7$	$\geqq 1.4 \times 10^5$	3.0
18-crown-6	K^+	27	1.1×10^4	3.4
18-crown-6	Na^+	180	6.3×10^3	3.4

This final solution contained 1 mM tris buffer, pH 7.4. The K_2 and K_3 values were calculated as described in the text. The value of k_{3b} was calculated as the maximal value of $(1/\tau) \times A_i/[I]$ obtained from the double reciprocal plot, where A_i is expressed in terms of numbers of binding sites on the inside surface. The maximal value of A_i is given by $(1/4)[PC](A_i/A_t)$ where A_i/A_t the fraction of binding sites on the inside surface (0.36; Table 10). The $1/\tau$ values were calculated as $0.69 \times (1/t_{\frac{1}{2}})$.

(McLaughlin, *et al.*, 1972) and it is possible that this complicates the behavior of the ionophore. The values of K_2 for (enniatin B)-K^+ are smaller than for the valinomycin and monactin K^+ complexation in keeping with the observation that enniatin B is less effective for transport through the mitochondrial membrane. We conclude from the above that the K_2 values measured in the phospholipid system do reflect the propensity of the $I-M^+$ complexes for transport through membranes.

Table 6 shows that the k_{3b} values for Na^+ complexes are equal to or smaller than those for K^+ for all of the ionophores. Ternary K^+ complexes are transported more rapidly than the corresponding ternary Na^+ complexes. We also note that the K_3 values for valinomycin and monactin have a Na^+/K^+ specificity. This behavior can be described loosely as a compensation of low K_2 values by high K_3 values such that the ion specificity for transport of the ternary complex becomes diminished. Below, we will discuss other published examples of diminution of ion specificity for valinomycin-induced transport in the presence of lipophilic anions and we will discuss evidence that these effects have a common basis.

Davis and Tosteson (1971, 1975) have presented evidence for the abolition of ion specificity of valinomycin for cation transport in lipid bilayers and red blood cell membranes in the presence of the organic anion, trinitro-*m*-cresolate. They also presented NMR experiments showing that the conformation of the Na^+ complex of valinomycin is dependent on both the solvent polarity and on the gegenanion. This is in distinction to the K^+ complex. The conformation of the Val-Na^+ tetraphenylboron$^-$ complex was judged equivalent to that of the Val-K^+ tetraphenylboron complex, whereas the ternary Br^-, CNS^- and trinitro-*m*-cresolate complexes showed evidence for cation-dependent conformation. This behavior can be understood in terms of direct participation by the less bulky anions in the cation complex. Our $^{23}Na^+$ nuclear magnetic resonance studies (Haynes *et al.*, 1971) give indirect evidence for ion pairing between monactin-Na^+ and (18-crown-6)-Na^+ and CNS^- in $CHCl_3$. This is deduced from our observations that the electronic environment of $^{23}Na^+$ in complexes in $CHCl_3$ is much less symmetrical than that of the complexes in methanol. If the anions are able to approach the complexed Na^+ more closely than they are able to approach the complexed K^+, then the Na^+/K^+ specificity of the K_3 values can be readily understood.

The k_{3b} values calculated here can be compared directly with the turnover numbers and rate constants reported for valinomycin in phos-

pholipid multilayers and lipid bilayers. Blok *et al.* (1974) calculated a turnover number of 328 ± 44 and $K_2 = 0.62 - 3.0\,M^{-1}$ and $K_3 = 20\,M^{-1}$ for valinomycin-induced KCNS permeability in phospholipid multilayers. Stark *et al.* (1971) and Benz *et al.* (1973) have reported first order rate constants of ca. $5 \times 10^4\,sec^{-1}$ and $1.5 \times 10^4\,sec^{-1}$ for the transfer of Val-K^+ across black lipid membranes made from phosphatidyl inositol and dipalmitoleoyl PC. The corresponding K_2 values were ca. $1\,M^{-1}$ and $0.4\,M^{-1}$. The turnover number for valinomycin in rat liver mitochondria is 2020 ± 430 (Haynes *et al.*, 1974).

The observation that the rate of ANS^- transport in the bilayer vesicle system is lower than that reported for black lipid membranes probably reflects either a difference of "membrane fluidity" of the two systems or differences in the easy of partitioning of the ionophore into the interior of the membrane. It has been shown by de Gier, Mandersloot and van Deenen (1968) that the nonelectrolyte permeability of liposomes increases with increasing degree of unsaturation and decreasing chain length. The lipid bilayer experiments were carried out at least 30 °C above their phase transition temperature, whereas the k_{3b} values of Table 6 are for a temperature 10° above T_m. The transport reaction has a large activation enthalpy ($\Delta H^{\ddagger} = 16.3 \pm 0.5$ kcal) and extrapolation of the measured rates to 53 °C (30 °C above T_m) gives a k_{3b} value of $310\,sec^{-1}$ in good agreement with the value of Blok *et al.* (1974). The remaining difference between this value and the values for mitochondria (Haynes *et al.*, 1974) and the lipid bilayer (Benz *et al.*, 1973) may be due to the presence of integral proteins in the former system and the presence of organic solvents in the latter system.

Our measured value of $\Delta H^{\ddagger}$ is in good agreement with the values measured by Johnson and Bangham (1969) and Blok *et al.* (1974) for $^{42}K^+$ flux and KCNS efflux (respectively) through phospholipid membranes.

Binding of Ionophores to the Membrane

We can make use of the catalytic influence of the ionophores on ANS^- transport to gain information about the rate at which the ionophores themselves communicate between the aqueous phase and the membrane. This can be accomplished in experiments in which the order of addition of the ionophore is varied. Comparison of the rates of ionophore-facilitated ANS^- transport, as measured in the previously

Table 7. Rate of ionophore binding to the vesicle membrane

Ionophore	Final ionophore concentration	$\Delta(1/t_{\frac{1}{2}})$ sec⁻1 (ionophore pretreatment)	$\Delta(1/t_{\frac{1}{2}})$ sec^{-1} (ionophore addition)	$\Delta(1/t_{\frac{1}{2}})$ sec^{-1} (partition experiment)
Valinomycin	2.82×10^{-7} M	3.93	2.25	0.110
Monactin	1.33×10^{-6} M	12.3	7.12	3.18
Enniatin B	4.75×10^{-6} M	6.51	4.1	3.42
18-crown-6	3.36×10^{-4} M	11.9	10.0	10.7

The experiment was carried out at 35 °C with 1 mM tris buffer, pH 7.4 with the following final concentrations of reactants: ANS⁻, 9×10^{-5} M; dimyristoyl-L-Lecithin, 3.52×10^{-4} M, 0.1 M KCl. In the repartition experiment half of the lipid was in each syringe. The experiment had the following configurations: Ionophore pretreatment; (vesicles + I) *vs.* (ANS + KCl); Ionophore addition; (vesicles) *vs.* (I + ANS⁻ + KCl); Repartition experiment, (vesicles + I − ANS + KCl) *vs.* (vesicles).

described experiments, with the rates obtained when the ionophore is added simultaneously with the ANS⁻, shows only small differences in the rate of ANS⁻ transport (Table 7). We conclude from this that all of the ionophores added to the aqueous phase are able to equilibrate with the membrane within 0.4 sec or less. The repartition experiments given in the third column of Table 7 were carried out in the following mixing configuration: Syringe A containing vesicles, ionophore, buffer and ANS⁻; syringe B containing vesicles and buffer. The rate of ANS⁻ transport is then measured for the vesicles originating from syringe B.

The above experiment can be interpreted to give information about the degree of ionophore binding to the vesicles in syringe A. If the rate in the third column is smaller than the rate in the second column, we have evidence that a substantial fraction of the total ionophore has been bound to the vesicles in syringe A and that this fraction is not transferred to the vesicles originating from syringe B within the $t_{\frac{1}{2}}$ measured in the repartition experiment. Since the rate of binding of the ionophore to the membrane was shown to be fast, the ratio of the values in column 3 to those of column 2 can be taken as an upper limit for the fraction of the total ionophore in the aqueous phase. We calculate the following lower limits for the partition coefficients and apparent binding constants based on phospholipid concentration: Valinomycin 2.0×10^5, 1.2×10^5 M^{-1}; monactin, 2.2×10^4, 1.3×10^4 M^{-1}; enniatin B, 1.1×10^4, 6.8×10^3 M^{-1}; 18-crown-6, $\ll2\times10^3$, $\ll1.1\times10^3$ M^{-1}. Analysis of the dependence of $\Delta(1/t_{\frac{1}{2}})\times A_i$ on the total lipid concentration for experiments of the type given in column 1 give values identical to those listed above. The

numbers cited above can, therefore, be considered as actual values of the partition coefficients and binding constants and we can estimate that the transfer of valinomycin, monactin or enniatin B between vesicles requires one sec or more. The partition coefficients above can be compared with the values of 2.5×10^4 for valinomycin and 6×10^3 for monactin for bulk decane phases containing PC (Stark & Benz, 1971).

Enhancement of ANS^- Binding due to Ionophore Complexation

In hopes of detecting and quantitating the complexation equilibrium of ionophores, we conducted a study of the effects of ionophore and cation addition on the fluorescence of ANS^- (Haynes, 1972). The rationale for these experiments was that ionophore complexation *on* or *in* the membrane would introduce a positive charge into the membrane which would increase the degree of ANS^- binding. This effect was actually observed with the neutral ionophores with M^+ in dimyristoyl and dipalmitoyl PC monolayer vesicles below their phase transition temperatures.

Ionophore addition gave an increase in ANS^- fluorescence which increased with increasing M^+ concentration. The rank order of effectiveness of the ionophores for this effect was valinomycin $\simeq$ monactin $>$ enniatin B $>$ 18-crown-6. This is in agreement with the rank order of transport efficiency induced by these agents when the latter quantity is not corrected for the ionophore partition equilibrium between the aqueous and membrane phase (Haynes *et al.*, 1974, Table 4). The reciprocal cation concentration giving rise to half-maximal effect was interpreted as the apparent binding constant for the cation on the ionophore. The apparent binding constants have the rank order $Rb^+ \geqq K^+ > Cs^+ > Na^+$ for all of the ionophores studied. The K^+/Na^+ specificity ratios were low (<10) and this finding was interpreted to mean that the complexes reported by the ANS^- method may differ from those which traverse the hydrophobic membrane interior in specific transport situation (Haynes, 1972). In the remainder of this section we will try to give this phenomenon a more quantitative treatment than given in our initial report (Haynes, 1972). This will be followed by a comparison with the cotransport model of Eq. (19).

The ionophore enhancement data are consistent with 1:1 stoichiometry between $I - M^+$ and the additional ANS^- bound when the assumption is made that the ANS^- bound in association with the

ionophore has a quantum yield approximately equal to that which is characteristic of an occupied binding site (ANS^--B). The fluorescence increase (ΔFl) is roughly proportional to the added ionophore concentration, and is relatively independent of the total lipid concentration[3]. This is illustrated in the following two examples: (*a*) The increase observed upon addition of ionophore to 1.3×10^{-4} M lipid (dimyristoyl PC) is only 30 % greater than the increase observed for 6.8×10^{-4} M lipid. (*b*) We have observed only ca. 15 % variation in $\Delta Fl/[I]$ for a 10-fold variation in $[ANS^-]$ (1×10^{-5} to 1×10^{-4} M).

Calculations of the extra ANS^- bound from ΔFl indicate a 1:1 stoichiometry, as is shown by the following example. Addition of 5×10^{-6} M valinomycin to 3.3×10^{-4} M dimyristoyl PC monolayer vesicles in the presence of 3×10^{-5} M ANS^- and 0.1 M KCl resulted in a 44 % enhancement of ANS^- fluorescence (Haynes, 1972). Under this condition, $[ANS^-]_b/[PC]=0.04$ before the addition of valinomycin (cf. Haynes, 1974, Fig. 1). The concentration of extra ANS^- bound upon the addition of 5×10^{-6} M valinomycin is calculated as 5.9×10^{-6} M. The agreement between these two numbers is within the experimental error.[4]

Similar analysis of all of our enhancement data at high $[MCl]$ has shown that the effect is best explained by the assumption of a 1:1 stoichiometry between $I-M^+$ and the extra ANS^- bound. We would expect a 1:1 stoichiometry to be held more strictly at low ionic strengths due to surface potential effects. We can thus interpret the enhancement ΔFl divided by its maximal value ΔFl_{max} as a direct measure of the degree of complexation of the ionophore according to

$$[I-M^+]/[I]_t=\Delta Fl/\Delta Fl_{max}. \tag{22}$$

ΔFl_{max} is obtained by extrapolation of double reciprocal plots to high M Cl concentrations.

3 We have observed in experiments conducted with $T<T_m$ that the results of valinomycin addition to bilayer vesicles were dependent upon the order of addition. Valinomycin addition to vesicles and ANS^- in absence of M^+ and subsequent addition of M^+ produced smaller fluorescence values than when the valinomycin was added in the presence of M^+. In all experiments reported here, the ionophores were added to vesicles preequilibrated with at least 2 mM M^+.

4 This interpretation (that Val-K^+ promotes ANS^- binding to the vesicle surface) has been criticized by Bessette and Seufert (1975) who reported that the quantum transfer efficiency between trapped acriflavine and externally added ANS^- is increased by the prescence of valinomycin. The ANS^- was assumed to be confined to the outside surface of the vesicles, and the increased quantum transfer efficiency was interpreted as the result at a thinning out of the membrane or reorientation of the bound ANS^-. The basic premise to the interpretation of these experiments seem to us, debatable, since our experiments show that ANS^- can cross the membrane in ca. 10 sec.

Table 8. Fluorescence enhancements of ionophore-cation combination of ANS^- fluorescence for dimyristoyl PC monolayer vesicles at 15 °C

Ionophore	Maximal fluorescence enhancements with cations ($M^{-1} \times 10^{-5}$)			
	Cs^+	Rb^+	K^+	Na^+
Valinomycin	0.57	0.48	1.05	0.89
Monactin	0.82	0.82	0.81	0.19
Enniatin B	0.035	0.059	0.130	0.063
Cyclohexyl 18-crown-6	0.013	0.008	0.013	0.019

The maximal fluorescence enhancement extrapolated from double reciprocal plots are given as the fractional increment of fluorescence upon ionophore addition divided by the ionophore concentration for 1.3×10^{-4} M lipid, 1.3×10^{-4} M ANS^-, and 0.1 M MCl.

Table 9. Apparent stability constants for $I-M^+$ on dimyristoyl PC monolayer vesicles at 15 °C

Ionophore	$K_{s(app)}\, M-1$			
	Cs^+	Rb^+	K^+	Na^+
Valinomycin	33	77	53	32
Monactin	67	100	83	14
Enniatin B	67	167	500	30
Cyclohexyl 18-crown-6	91	111	53	36

The apparent stability constants were determined from double reciprocal plots of the fluorescence increments upon ionophore additions *vs.* cation concentration under experimental conditions otherwise identical to those of Table 8.

The maximal fluorescence enhancements and apparent stability constants for complex formation of several ionophore combinations are shown in Tables 8 and 9 for dimyristoyl PC monolayer vesicles below their phase transition temperature. In most cases, we obtained identical data for dipalmitoyl PC monolayer vesicles. Although we observed some difference in the size of the enhancement effect for monolayer and bilayer vesicles, the dependencies on the ionophore and cation and on their concentrations were similar if not identical for the two preparations. The experiments of Tables 8 and 9 were also carried out using 2-*p*-toluidinylnaphthalene-6-sulfonate (TNS^-) with qualitatively similar results. The cation and ionophore specificity results thus cannot be highly dependent on special steric features of the fluorescent anion probe.

The values of maximal fluorescence enhancement of Table 8 show low ion specificity. The values for valinomycin and monactin range over a factor of 2. We interpret these differences to be the result of small differences in the quantum yield of the $I-M^+$-associated ANS$^-$ species. This could arise from differences in the degree of shielding of the fluorophore from water. The fluorescence enhancements for enniatin B and 18-crown-6 are significantly smaller. Experiments in which the total lipid concentrations were varied showed that valinomycin and monactin are tightly bound to the membrane whereas enniatin B and 18-crown-6 are weakly bound. The low enhancement values are partially due to the low degree of binding of the latter two to the membrane.

Table 9 shows that the apparent stability constants, K_{app}[5], of the $I-M^+$ complexes have small but significant ion specificities. The rank order of ion specificity of valinomycin and monactin is $Rb^+ > K^+ > Cs^+ > Na^+$. The ion specificities of enniatin B and 18-crown-6 are $K^+ > Rb^+ > Cs^+ > Na^+$ and $Rb^+ > Cs^+ > K^+ > Na^+$, respectively. In the latter case it is uncertain whether the results were influenced by complexation in the aqueous phase (McLaughlin *et al.*, 1972). The actual values of K_{app} are at least 5 times larger than the corresponding values of K_2 (Table 6).

In a previous communication (Haynes, 1972) we proposed that below the phase transition temperature, the ionophores are trapped on the membrane surface and that above the phase transition temperature they are able to penetrate the hydrocarbon chain region. We would thus consider the high K_{app} values to be characteristic of the ionophore on the membrane surface. The values of K_2 are expected to be lower than the K_{app} values if the former are thought to represent complexation in a more hydrophobic region of the membrane since, by analogy to the two phase extraction system (Haynes & Pressman, 1974), the latter complexes should have lower stability constants when M^+ is referred back to the aqueous phase. In the two phase extraction system the stability constant (K_{3a} in notation of Haynes & Pressman, 1974) decreases with decreasing polarity of the organic phase.

---

5 We cannot ascribe the same meaning to the apparent binding constant as $K_{app(M^+)}$ in Eq. (21) because the value was not observed to depend upon the ANS$^-$ concentration in the range 10^{-5} to 10^{-4} M. The model of Eq. (19) is therefore inappropriate. An alternative model would explain the stoichiometric relationship between extra ANS$^-$ binding and $I-M^+$ complex formation as the result of a strong electrostatic coupling between those species such that the surface charge and surface potential do not change value after the addition of the ionophore. However, this model also predicts a dependence of the apparent binding constant on the free ANS$^-$ concentration, as mediated through membrane surface potential effects on the distribution of the complexing cations in the electric double layer. The values of K_{app} are thus presented without an appropriate model.

Electrostatic Interactions

We can use our ability to differentiate between ANS^- bound to the inside and outside surfaces of the vesicle to determine whether the surfaces have identical dependencies of surface potential on ionic strength and surface charge. The relationship between these parameters appropriate for the outside surface has been studied with monolayer vesicles (Haynes, 1974). The surface potentials determined by the binding equilibrium of ANS^- were smaller than those calculated using the Gouy-Chapman theory, and the discrepancy was attributed to discreteness-of-charge effects on the membrane surface (Haynes, 1974). The quantitative treatment given below is based on simplifying assumptions of high surface charge density and surface potential.

For the case of low degrees of saturation of the ANS^- binding sites, the amount of ANS^- binding can be described as a linear isotherm such that

$$[ANS^-]_b = [B]_t K_{10} f(\sigma) [ANS^-] \tag{23}$$

where $[B]_t$ is the total number of binding sites on the surface under consideration, K_{10} is the "chemical" binding constant for ANS^- on these sites in absence of electrostatic interaction, and $f(\sigma)$ is an electrostatic factor equal to $\exp(e\Psi_0/kT)$. For high negative values of surface charge and potential, and a 1:1 electrolyte in the medium (MCl) the Gouy-Chapman equation predicts

$$\exp(e\Psi_0/kT) = \frac{[M^+]\varepsilon kT}{\sigma^2 2\pi} \tag{24}$$

where ε is the dielectric constant of the medium, k is the Boltzmann constant, and σ is the density of the fixed negative charge on the membrane surface.

We will derive equations predicting the behavior of ANS^- binding *vs.* ionic strength for two limiting cases. In case *A*, there is a high degree of ANS^- binding to a neutral membrane and the surface charge density is given as

$$\sigma = k_1 [ANS^-]_b \tag{25}$$

where k_1 is a constant. Combining Eqs. (23), (24) and (25) under the assumption that $f(\sigma)$ is given correctly by the Gouy-Chapman theory gives

$$[ANS^-]_b = ([B]_t K_{10} \varepsilon k T / k_1^2 2\pi)^{1/3} [ANS^-]^{1/3} [M^+]^{1/3} \tag{26}$$

which predicts that the degree of ANS^- binding will have a 1/3rd power dependence on the monovalent cation concentration in the medium.

In case *B*, there is an existing high negative surface charge on the membrane such that changes in ANS^- binding do not affect the surface potential significantly. In this case we have σ = fixed charge, and combination with Eqs. (23) and (24) under the assumption that $f(\sigma)$ is given correctly by the Gouy-Champman theory predicts

$$[ANS^-]_b = ([B]_t K_{10} \varepsilon kT/\sigma^2 2\pi)\ [ANS^-][M^+] \tag{27}$$

with a first power dependence on ionic strength.

Fig. 9 shows that the inner and outer surfaces of the vesicle have markedly different ionic strength dependencies of their ANS^- binding. Under the assumptions of high surface potential experienced at the ANS^- binding site due to the contribution of PA^-, application of the Gouy-Chapman equation in the form of Eq. (27) would predict a slope of 1.0. The observed slopes of 0.4 (outer surface) and 0.6 (inner surface) are significantly smaller. These observations lend further support to our

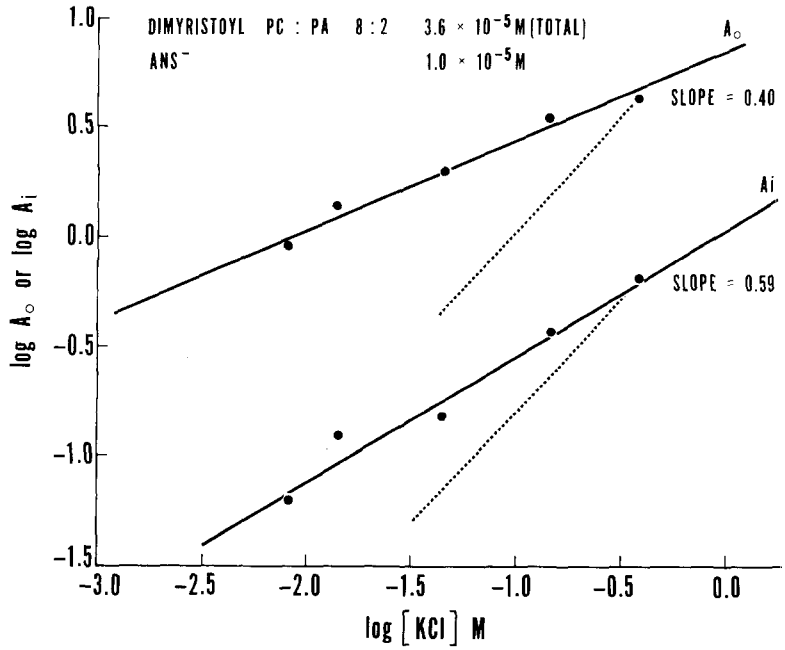

Fig. 9. The ionic strength dependence of ANS^- binding to the inside and outside layers of dimyristoyl PC/PA 8:2 vesicles. The dotted lines indicate a slope of 1.0. Reaction conditions: Total lipid concentration 3.6×10^{-5} M, 1.0×10^{-5} M ANS^-, 1 mM tris, pH 7.4, 35 °C. Identical results were obtained in the presence of 1.3×10^{-6} M valinomycin

Table 10. Ionic strength dependence of ANS^- binding

Lipid	Slope A_i		Slope A_o		A_i/A_o
	Observed	Expected	Observed	Expected	
Dimyristoyl PC	0.35	0.33	0.29	0.33	0.63
Dimyristoyl PC/PA 8:2	0.60	1.0	0.40	1.0	0.14
Dimyristoyl PC/cholesterol	0.30	0.33	0.20	0.33	0.095
Dimyristoyl PC/PE 8:2	0.36	0.33	0.14	0.33	0.25

The values are for $3.5 \times M^{-5}$ M lipid concentration and 9.6×10^{-5} M ANS^- at 35 °C. The values of "slope" are the slopes of plots of $\log A$ *vs.* $\log [I]$, where I is the ionic strength. The values of A_i/A_o are for 0.47 M KCl, and represent the maximal values measured. Identical results were obtained with and without valinomycin.

conclusion that the potential sensed by ANS^- at its binding site can be considerably smaller than that predicted by the Gouy-Chapman theory (Haynes, 1974). We have suggested earlier that this difference is the result of discreteness-of-charge effects on the membrane surface. We have also obtained additional evidence for a smaller than predicted surface potential from studies in which the ionic strength dependence of H^+ binding to PA^- incorporated into PC vesicles was measured (Haynes, *unpublished*).

Table 10 compares values of the slope for ANS^- binding on both surfaces with those expected from Eq. (26). Our previous study (Haynes, 1974) showed that the surface potentials produced by ANS^- binding and sensed by ANS^- binding to monolayer vesicles are smaller in absolute value than those predicted by the Gouy-Chapman theory. The ionic strength dependence of ANS^- binding to the outside surface as indicated by the slope values in Table 10 for the PC/PE and PC/cholesterol mixtures are significantly smaller than for vesicles made from pure PC. This can be expected since the lipid mixtures have a lower density of binding sites such that the condition of high surface potential is not fulfilled throughout the whole range of cation concentration.

The slope of the log-log plot for the inwardly-facing surface is larger than that for the outwardly-facing surface in all cases shown in Table 10. In three cases it is slightly higher than predicted by Eq. (26). This is an intuitively-expected result of the effect of the vesicle geometry on the potential distribution. A double layer of counterions facing an inwardly-facing surface will be more crowded and the drop in potential in the

direction perpendicular to the membrane will be less steep. Larger surface potentials will thus be expected.[6]

Inside vs. Outside Distribution in Mixed Lipid Systems

Recent evidence for an asymmetric distribution of phospholipids across the erythrocyte membrane (Verkliej *et al.*, 1973; Marinetti & Love, 1974) has given rise to the question of whether such phenomena have metabolic or thermodynamic origins. Studies with phospholipid vesicles have shown that asymmetric distributions of phospholipids can occur, indicating a thermodynamic basis for this phenomena, at least for membranes with small radii of curvature. Michaelson, Horwitz and Klein, (1973) have used nuclear magnetic resonance techniques to show that phosphatidyl glycerol (PG) concentrates on the inside surface of vesicles prepared from PG-PC mixtures. Huang *et al.* (1974) have studied vesicles prepared from cholesterol-PC mixtures with a variety of physical techniques and have concluded that cholesterol distributes preferentially on the inside surface. Litman (1973) has used data on the inside-outside distribution of PE in vesicles made from PE/PC mixtures and has made calculations using estimates of the vesicle size to demonstrate a tendency for PE to be concentrated on the inside surface. The following discussion will show how our ability to distinguish between fluorescent signals arising from the inside and outside surfaces of the vesicles allows us to make deductions about their mole fractional composition in mixed lipid systems. Our considerations can be applied as a method, when the dependencies of the number of ANS^- binding sites on mole ratio established in earlier studies of monolayer vesicles are used (Haynes & Staerk, 1974).

It is first necessary to prove our assertion that the A_i/A_o values are consistent with ratios of surface areas expected for vesicles based on their

6 Conversely, an attenuation of the membrane surface potential would be expected for the outwardly-facing surface. This occurs when the ionic strength-dependent Debye-Hückel length (K^{-1}) becomes comparable to the radius of curvature at low ionic strengths. The magnitude of this effect has been evaluated by Loeb, Overbeek and Wiersema, (1961). We have made calculations using values tabulated in Table 1 of their book to determine how much the surface potential should be attenuated by the effect of curvature under the experimental conditions of this and of our previous publication. For 2.5 mM ionic strength ($K^{-1}=62$ Å) with $R=125$ Å with a surface charge of one per phospholipid molecule, the membrane surface potential is attenuated only about 20 %. A series of calculations has shown that this is the largest effect to be expected under our experimental conditions.

electron microscopically determined radii. The outer radius, r_o, of a spherical vesicle should be given as

$$r_o = d/(1 - x^{\frac{1}{2}}) \tag{28}$$

where x is the ratio of inside to outside surface area and d is the membrane thickness. Applying this to dimyristoyl PC vesicles using the A_i/A_o $(=x)$ values given in Table 10 and using $d = 40$ Å (*cf.* Träuble & Haynes, 1971) gives $r_o = 190$ Å. This value is within the range of values determined by electron microscopy on similar preparations (125 Å, Huang, 1969; 250 Å, Papahadjopoulos & Miller, 1967) and can be considered as an average radius for our preparation.

We note that the A_i/A_o values in the mixed lipid systems are much lower than the value for dimyristoyl PC and that this can be attributed to two dependencies: (a) The radius dependence given in Eq. (28) and (b) the dependence of the number of binding sites in a mixture on its composition. We showed that lipids (L) which in the pure form do not support ANS^- binding (PA^-, PE and cholesterol) will, upon incorporation into a PC membrane, destroy ANS^- binding sites, (B) according to

$$[B]/[B]_{PC} = (1 - f_L)^4 \quad (= f_{PC}^4). \tag{29}$$

Here B is the number of binding sites per lipid molecule in the mixture, $[B]_{PC}$ is the number of binding site per molecule of PC in the pure form (0.25), and f_L and f_{PC} are the mole fractions of the nonsupportive lipid and the PC, respectively. While either the radius dependence or the mole fraction dependence could, in principle, be responsible for the observation that the A_i/A_o values for the mixed lipid systems are lower than for PC, only the mole fraction dependence gives a qualitatively and quantitatively reasonable description of the system. Johnson (1973) has shown that the incorporation of PA^- or cholesterol into lecithin membranes increases the vesicle radius. We would, therefore, expect A_i/A_o values greater than for PC if the former were determined according to Eq. (28). Furthermore, if we assume that the A_i/A_o values are determined according to Eq. (28), then we arrive at unreasonably low values of r_o (PC/PA, 64 Å; PC/cholesterol, 58 Å; PC/PE, 80 Å).

We have, therefore, analyzed the data according to the assumption that the dependence of Eq. (29) is the sole determinant of the A_i/A_o values, and that all of the radii are equal to that of dimyristoyl PC vesicles. The latter conclusion will be examined at the end of the following analysis.

Under the above assumptions, the mole fraction PC in the inside and outside surfaces can be calculated from A_i/A_o according to

$$f_{PC_o}/f_{PCi} = (x_{obs}/x_{ideal})^{\frac{1}{4}} \tag{30}$$

where x_{obs} is the ratio of A_i/A_o for the lipid mixture, and x_{ideal} is the corresponding quantity for the PC vesicles. The mole fractions of all components for the inside and outside surfaces can then be calculated using

$$(A_i/(A_o+A_i))\, f_{PCi} + (A_o/(A_o+A_i))\, f_{PCo} = f_{PCt} \tag{31}$$

and

$$(A_i/(A_o+A_i))\, f_{Li} + (A_o/(A_o+A_i))\, f_{Lo} = f_{Lt}, \tag{32}$$

where f_{Lt} and f_{PCt} represent the total mole fractions of the nonsupportive lipid and PC, respectively, and where the $A_i/(A_o+A_i)$ ratios are those for pure PC vesicles. The results of this analysis, tabulated in Table 11, show an approximate two-fold preference of cholesterol and PE for the inside surface and an approximate four-fold preference of PA^- for the inside surface. The cholesterol result is in agreement with the results of Huang *et al.* (1974) who have given evidence that egg PC bilayer membranes with overall mole fractions of cholesterol above 30 % have a larger mole fraction of cholesterol on the inner half of the bilayer. These workers interpreted the preference as the result of replacement of PC molecules with unsaturated chains by cholesterol on the inner layer. Our finding of a similar result with saturated dimyristoyl PC indicates that the preference can be understood as the result of the effect of cholesterol insertion to space out the polar head groups. This could attenuate steric

Table 11. Calculated inside outside distribution in mixed lipid vesicles[a]

Lipid mixture	Mole fraction				
	PC_o	$Lipid_o$	PC_i	$Lipid_i$	$Lipid_i/Lipid_o$
Dimyristoyl PC cholesterol 2:1	0.78	0.22	0.50	0.50	2.3 (±0.2)
Dimyristoyl PC/PE 8:2	0.87	0.13	0.69	0.31	2.4 (1.9 – 3.5)[b]
Dimyristoyl PC/PA 8:2	0.913	0.087	0.62	0.38	4.4 (1.6 – 6.7)[b]

[a] Calculations were made using the A/A_o date of Table 10 and Eqs. (30), (31) and (32), assuming uniform vesicle radius, defined by the A_i/A_o value of dimyristoyl PC. Pertinent experimental conditions are given in Table 10.

[b] Outermost limits of systematic error in the analysis as estimated on the assumption that A_i/A_o values show a ±50 % deviation from their expected dependence on the mole fraction values.

and dipolar electrostatic repulsive interactions of the PC polar head groups on the more crowded inside surface to a greater degree than on the less crowded outside surface.[7]

The preference of PE for the inside surface is in agreement with the findings of Litman (1973). He compared the tendency of PE to be stabilized at the inside surface of vesicles containing PC and PE to the tendency of the latter to form hexagonal phases when occurring in the pure form. We have cited evidence (Haynes & Staerk, 1974) for a self-associating tendency of PE polar head groups, possibly mediated through head-to-tail hydrogen bonding. Such associative tendencies would stabilize the PE on the inside surface and destabilize the PE on the outside surface.

The value of A_i/A_o for PC/PA 8:2 membranes was the influenced to only a small extent by the electrostatic surface potential, and its low value indicates a preference of PA^- for the inside surface. This preference cannot be understood in simple terms. Calculations of electrostatic energy should suggest a preference for the outside surface (Israelachvili, 1973) and nuclear magnetic resonance studies using a paramagnetic broadening technique (Michaelson *et al.*, 1973) have shown that phosphatidyl glycerol (PG^-) shows a two-fold preference for the outside surface. We note, however, that the glycerol portion of the PG^- molecule represents a possible source of steric hindrance to inwardly-directed packing and that this influence is absent in PA^-. Our recent temperature-jump rapid kinetic studies on the kinetics of Ca^{2+} binding in mixed PC/PA systems indicate that the choline head-group may even occupy space very close to the phosphate residue of the PA^-, since Ca^{2+} binding to the latter is two orders of magnitude slower than expected for the case of diffusion control (Haynes, 1977). This could be interpreted as the result of an associative tendency of PC and PA, and the preference of PA for the inside surface could be explained if this associative tendency were stronger on the inside surface.

We can also derive evidence that PA^- has less sterically-hindered head group interactions than PG^- and PC from a consideration of the differences in phase transition temperatures of these lipids in the pure form. Jacobson and Papahadjopoulos (1975) determined T_m values of

7 This qualitative statement can be bolstered up by geometric calculations if simple models are used. If the polar head group is considered as an 8-Å line oriented perpendicular to the surface of a vesicle with $r_o = 190$ Å and with 8 Å between the polar head groups at their centers, then the tips of the inwardly oriented polar head groups will be 7.6 Å apart, and the tips of the outwardly oriented polar head groups will be 8.3 apart

42 °C, 41 °C and 67 °C for dipalmitoyl PC, PG^- and PA^-, respectively. If we consider the hydrocarbon chain spacing and packing to be independent of the type of polar head group above and below the phase transition temperature, then the differences in T_m must be due to differences in polar head group contribution to the free energy connected with the process of lateral expansion of the membrane. The comparison shows that PA^-, despite its negative charge, is more stabilized in the condensed form than is the zwitterionic PC, and would thus be expected to favor the inside surface of the bilayer. The equality of the T_m values for PG^- and PC would indicate that the sums of the changes in electrostatic plus steric interaction energies for those phospholipids are equal.

Conclusions

Our findings include four points of relevance to the interpretation of the behavior of ANS^- and similar charged surface probes in biological membranes: (a) The uncatalyzed transport of ANS^- through phospholipid membranes requires 10–100 sec, and similar times would be required for transport through phospholipid regions of biological membranes. (b) If faster permeation were observed in biological membranes, then this could be taken as evidence for discontinuities in the hydrophobic region due to the influence of membrane protein. Alternatively it could be taken as evidence that the ANS^- transport involves a permeability system intrinsic to the membrane. (c) The ANS^- transport seems to rely on ion pair formation, and its rate in the presence of neutral ionophores appears to be insensitive to the membrane potential in our system and may not show sensitivity in other systems. (d) This last comment implies that fluorescence transients arising from ANS^- in biological membranes with half-times of less than one sec (in absence of ionophores) are probably not due to ANS^- transport. They may have their origins in changes in quantum yield or binding as influenced by rearrangement of membrane components or in alterations of the charge or potential of the membrane surface.

This work was supported by Grant 1 P01 HL 16117-01 from the National Institutes of Health and by the Florida Heart Association. The previous two papers of this series (Haynes & Staerk, 1974; Haynes, 1974) were also written under the tenure of the grant. The portions of this work dealing with the fluorescence enhancement effects of the ionophores were supported by a postdoctoral fellowship from the Damon Runyon Fund

for Cancer Research and were carried out at the Max-Planck-Institut für biophysikalische Chemie, Göttingen, Germany. We thank Professor Manfred Eigen for the sponsorship of and Mr. Jörg Ronnenberg for technical assistance in this portion of the study. We also thank Mr. Gerard Laumen for help with the preparation of the manuscript.

Finally, we thank Dr. A Waggoner and Dr. K. Jacobson and the two referees engaged by the Journal for their helpful criticism and constructive advice.

Note Added in Proof

It has been brought to our attention that biphasic fluorescent responses upon ANS^- addition have been reported by Fortes and Hoffman (Fortes, P.A.G. & Hoffman, J.F. (1971) *J. Membrane Biol.* **5**:154–168) for human red cell ghosts.

References

Azzi, A., Chance, B., Radda, G.K., Lee, C.P. 1969. A fluorescence probe of energy-dependent structure changes in fragmented membranes. *Proc. Nat. Acad. Sci. USA* **62**:612

Bakker, E.P., Dam, K. van. 1974. Influence of diffusion potentials across liposomal membranes on the fluorescence intensity of 1-anilino-8-naphthalenesulfonate. *Biochim. Biophys. Acta* **339**:157

Benz, R., Stark, G., Janko, K., Läuger, P. 1973. Valinomycin-mediated ion transport through neutral lipid membranes: Influence of hydrocarbon chain length and temperature. *J. Membrane Biol.* **14**:339

Bessette, F., Seufert, W.D. 1975. Increase in fluorescence energy transfer across lipid bilayers induced by valinomycin. *Biochim. Biophys. Acta* **373(1)**:10

Blok, M.C., Gier, J. de, Van Deenen, L.L.M. 1974. Kinetics of the valinomycin-induced potassium ion leak from liposomes with potassium thiocyanate enclosed. *Biochim. Biophys. Acta* **367**:210

Chapman, D. 1965. The Structure of Lipids. Methuen, London

Chapman, D., Byrne, P., Shipley, G.G. 1966. Physical studies of phospholipids. I. Solid state and mesomorphic properties of some 2,3-diacyl-DL-phospatidylethanolamines. *Proc. R. Soc. London A* **290**:115

Chapman, D., Williams, R.M., Ladbrooke, B.D. 1967. Physical studies of phospholipids. VI. Thermotropic and lyotropic mesomorphism of some 1,2-diacylphosphatidylcholines (lecithins). *Chem. Phys. Lipids* **1**:445

Ciani, S., Eisenman, G., Szabo, G. 1969. A theory for the effects of neutral carriers such as the macrotetralide actin antibiotics on the electric properties of bilayer membranes. *J. Membrane Biol.* **1**:1

Conti, F., Tasaki, I., Wanke, E. 1971. Fluorescence signals in ANS-stained squid giant axons during voltage-clamp. *Biophysik* **8**:58

Cornelius, G., Gärtner, W., Haynes, D.H. 1974. Cation complexion by valinomycin- and nigericin-type ionophores registered by the fluorescence signal of Tl^+. *Biochemistry* **13**:3052

Davis, D.G., Tosteson, D.C. 1971. Interaction between valinomycin and K^+, Na^+, and anions in $CDCl_3$ and hexane. *Biophys. J.* **11**:310*a*

Davis, D.G., Tosteson, D.C. 1975. Nuclear magnetic resonance studies of the interactions of anions and solvent with cation complexes of valinomycin. *Biochemistry* **14**:3962

Devaux, P., McConnell, H.M. 1972. Lateral diffusion in spin-labelled phosphatidylcholine multilayers. *J. Am. Chem. Soc.* **94**:4475

Eisenman, G., Ciani, S., Szabo, G. 1969. The effects of the macrotetralide actin antibiotics on the equilibrium extraction of alkali metal salts into organic solvents. *J. Membrane Biol.* **1**:294

Gains, N., Dawson, A.P. 1975. Transmembrane electrophoresis of 8-anilino-1-naphthalenesulfonate through egg lecithin liposome membranes. *J. Membrane Biol.* **24**:237

Gier, J. de, Mandersloot, J.G., Deenen, L.L.M. van. 1968. Lipid composition and permeability of liposomes. *Biochim. Biophys. Acta* **150**:666

Haynes, D.H. 1972. Detection of ionophore-cation complexes on phospholipid membranes. *Biochim. Biophys. Acta* **255**:406

Haynes, D.H. 1974. 1-anilino-8-naphthalenesulfonate: A fluorescent indicator of ion binding and electrostatic potential on the membrane surface. *J. Membrane Biol.* **17**:341

Haynes, D.H. 1977. Metal-ligand interactions in organic and biochemistry. *In:* 9th Jerusalem Symposium. B. Pullman, editor. J. Reidel Publishing, Dordrecht-Holland (*in press*)

Haynes, D.H., Pressman, B.C. 1974. Two-phase partition studies of alkali cation complexation by ionophores. *J. Membrane Biol.* **18**:1

Haynes, D.H., Pressman, B.C., Kowalsky, A. 1971. A nuclear magnetic resonance study of $^{23}Na^{+}$ complexing by ionophores. *Biochem.* **10**:852

Haynes, D.H., Staerk, H. 1974. 1-anilino-8-naphthalenesulfonate: A fluorescent probe of membrane surface structure, composition and mobility. *J. Membrane Biol.* **17**:313

Haynes, D.H., Wiens, T., Pressman, B.C. 1974. Turnover numbers for ionophore-catalyzed cation transport across the mitochondrial membrane. *J. Membrane Biol.* **18**:23

Huang, C. 1969. Studies on phosphatidylcholine vesicles. Formation and physical characteristics. *Biochemistry* **8**:344

Huang, C.H., Sipe, J.P., Chow, S.T., Martin, R.B. 1974. Differential interaction of cholesterol with phosphatidylcholine on the inner and outer surface of lipid bilayer vesicles. *Proc. Nat. Acad. Sci. USA* **71**:359

Israelachvili, J.M. 1973. Theoretical considerations on the asymmetric distribution of charged phospholipid molecules on the inner and outer layers of curved bilayer membranes. *Biochim. Biophys. Acta* **323**:659

Jacobson, K., Papahadjopoulos, D. 1975. Phase transition and phase separation in phospholipid membranes induced by changes in temperature, pH, and concentration in bivalent cations. *J. Biochem.* **14(1)**:152

Jacobson, K., Papahadjopoulos, D. 1976. Effect of a phase transition on the binding of 1-anilino-8-naphthalenesulfonate to phospholipid membranes. *Biophys. J.* **16**:549

Johnson, S.M. 1973. The effect of charge and cholesterol on the size and thickness of sonicated phospholipid vesicles. *Biochim. Biophys. Acta* **307**:27

Johnson, S.M., Bangham, A.D. 1969. Potassium permeability of single compartment liposomes with and without valinomycin. *Biochim. Biophys. Acta* **193(1)**:82

Ketterer, B., Neumcke, B., Läuger, P. 1971. Transport mechanism of hydrophobic ions through lipid bilayer membranes. *J. Membrane Biol.* **5**:225

Ladbrooke, B.D., Chapman, D. 1969. Thermal analysis of lipids, proteins and biological membranes. Review and summary of some recent studies. *Chem. Phys. Lipids* **3(4)**:304

Lansman, J., Haynes, D.H. 1975. Kinetics of Ca^{++}-triggered membrane aggregation reaction of phospholipid membranes. *Biochim. Biophys. Acta.* **394**:335

Litman, B.J. 1973. Lipid model membranes: Characterization of mixed phospholipid vesicles. *Biochemistry* **12**:2545

Loeb, A.L., Overbeek, J.T.G., Wiersema, P.H. 1961. The electrical double layer around a spherical colloid particle. p. 19. M.I.T. Press, Cambridge

Marinetti, G.V., Love, R. 1974. Extent of cross-linking of amino-phospholipids neighbours in the erythrocyte membrane as influenced by the concentration of difluorodinitrobenzene. *Biochem. Biophys. Res. Commun.* **61**:30

McLaughlin, S.G.A., Szabo, G., Ciani, S., Eisenman, G. 1972. The effects of a cyclic polyether on the electrical properties of phospholipid bilayer membranes. *J. Membrane Biol.* **9**:3

Michaelson, D.M., Horwitz, A.F., Klein, M.P. 1973. Transbilayer asymmetry and surface homogeneity of mixed phospholipid in cosonicated vesicles. *Biochemistry* **12**:2637

Papahadjopoulos, D., Miller, N. 1967. Phospholipid model membranes. I. Structural characteristics of hydrated liquid crystals. *Biochim. Biophys. Acta* **135**:624

Papahadjopoulos, D., Poste, G., Schaeffer, B.E., Bail, W.J. 1974. Membrane fusion and molecular segregation in phospholipid vesicles. *Biochim. Biophys. Acta* **352**:10

Papahadjopoulos, D., Watkins, J.C. 1969. Phospholipid model membranes. II. Permeability properties of hydrated liquid crystals. *Biochim. Biophys. Acta* **135**:639

Parsegian, A. 1969. Energy of an ion crossing a low dielectric membrane: Solutions to four relevant electrostatic problems. *Nature (London)* **221**:844

Phillips, M.C., Williams, R.M., Chapman, D. 1969. On the nature of hydrocarbon chain motions in lipid liquid crystals. *Chem. Phys. Lipids* **3**:234

Sims, P.J., Waggoner, A.S., Wang, C.H., Hoffman, J.F. 1974. Studies on the mechanism by which cyanine dyes measure membrane potential in red blood cells and phosphatidylcholine vesicles. *Biochemistry* **13**:3315

Stark, G., Benz, R. 1971. The transport of potassium through lipid bilayer membranes by the neutral carriers valinomycin and monactin. Experimental studies to a previously proposed model. *J. Membrane Biol.* **5**:133

Stark, G., Ketterer, B., Benz, R., Läuger, P. 1971. The rate constants of valinomycin-mediated ion transport through thin lipid membranes. *Biophys. J.* **11**:981

Szabo, G., Eisenman, G., Ciani, S. 1969. The effects of the macrotetralide actin antibiotics on the electrical properties of phospholipid bilayer membranes. *J. Membrane Biol.* **1**:346

Träuble, H., Grell, E. 1971. The formation of asymmetrical spherical lecithin vesicles. *Neurosci. Res. Prog. Bull.* **9(3)**:373

Träuble, H., Haynes, D.H. 1971. The volume change in lipid bilayer lamellae at the crystalline-liquid crystalline phase transition. *Chem. Phys. Lipids* **7**:324

Träuble, H., Sackmann, E. 1972. Studies of the crystalline-liquid crystalline phase transition of lipid model membranes. III. Structure of a steroid-lecithin system below and above the lipid-phase transition. *J. Am. Chem. Soc.* **94**:4499

Tsong, T.Y. 1975*a*. Effect of phase transition on the kinetics of dye transport in phospholipid bilayer structures. *Biochemistry* **14**:5409

Tsong, T.Y. 1975*b*. Transport of 1-anilino-8-naphthalenesulfonate as a probe of the effect of cholesterol on the phospholipid bilayer structures. *Biochemistry* **13**:5415

Vanderkooi, J., Martonosi, A. 1971*a*. Sarcoplasmic reticulum. XII: The interaction of 8-anilino-1-naphthalenesulfonate with skeletal muscle microsomes. *Arch. Biochem Biophys.* **144**:87

Vanderkooi, J.M., Martonosi, A. 1971*b*. Sarcoplasmic reticulum. XIII. Changes in the fluorescence of 8-anilino-1-naphthalenesulfonate during Ca^{2+} transport. *Arch Biochem. Biophys.* **144**:99

Verkleij, A.J., Zwaal, R.F.A., Roelofsen, B., Comfeurius, P., Kastelijn, D., Deenen, L.L.M van. 1973. The asymmetric distribution of phospholipids in the human red cel membrane. A combination study using phospholipases and freeze-etch electron microscopy. *Biochim. Biophys. Acta* **323**:178

Yi, P.N., MacDonald, R.C. 1973. Temperature-dependence of optical properties o aqueous dispersions of phosphatidylcholine. *Chem. Phys. Lipids* **11**:114